# Dynamics and Control of Flexible Composite Robotic Manipulators Based on Finite Element Method

A THESIS SUBMITTED IN THE PARTIAL FULFILLMENT OF

THE REQUIREMENTS FOR THE DEGREE OF

**Master of Technology (Research)**

**In**

**Mechanical Engineering**

**(Specialization: Machine Design and Analysis)**

**By**

**JEFRIN JOSE P.**

**612ME307**


Department Of Mechanical Engineering
National Institute of Technology Rourkela
Rourkela, Odisha, India – 769008
January, 2015

# Dynamics and Control of Flexible Composite Robotic Manipulators Based on Finite Element Method

A THESIS SUBMITTED IN THE PARTIAL FULFILLMENT OF

THE REQUIREMENTS FOR THE DEGREE OF

**Master of Technology (Research)**

**In**

**Mechanical Engineering**

**(Specialization: Machine Design and Analysis)**

**By**

**JEFRIN JOSE P.**

**612ME307**

**Under the supervision of**

**Dr. Tarapada Roy**


Department Of Mechanical Engineering
National Institute of Technology Rourkela
Rourkela, Odisha, India – 769008
January, 2014

# DECLARATION

I hereby declare that this submission is my own work and that, to the best of my - knowledge and belief, it contains no material previously published or written by another person nor material which to a substantial extent has been accepted for the award of any other degree or diploma of the university or other institute of higher learning, except where due acknowledgement has been made in the text.

**(JEFRIN JOSE P.)**
**Date: 22-01-2015**


**NATIONAL INSTITUTE OF TECHNOLOGY ROURKELA**

# CERTIFICATE

This is to certify that the thesis entitled, **"Dynamics and Control of Flexible Composite Robotic Manipulators Based on Finite Element Method"** being submitted by **Mr. JEFRIN JOSE P.** in partial fulfilment of the requirements for the award of **"MASTER OF TECHNOLOGY (RESEARCH)"** Degree in **"MECHANICAL ENGINEERING"** with specialization in **"MACHINE DESIGN AND ANALYSIS"** at the National Institute of Technology Rourkela (India) is an authentic work carried out by him under my supervision.

To the best of our knowledge, the results embodied in the thesis have not been submitted to any other University or Institute for the award of any Degree or Diploma.

Date:

**Dr. TARAPADA ROY**
Department of Mechanical Engineering
National Institute of Technology
Rourkela-769008

# ACKNOWLEDGEMENT

I thank God Almighty for being a tower of strength and guiding force, giving me faith and courage to carry on even during difficult times.

First and foremost I offer my sincerest gratitude and respect to my supervisor Dr. Tarapada Roy, for his invaluable guidance and suggestions to me during my study. I consider myself extremely fortunate to have had the opportunity of associating myself with him for two and half years. This thesis was made possible by his patience and persistence.

I am thankful to Prof. Sunil Kumar Sarangi, Director of National Institute of Technology, for giving me an opportunity to be a part of this prestigious institute of national importance. I am thankful to Prof. Siba Sankar Mohapatra, the Head of the Department, Department of Mechanical Engineering, for his moral support and valuable suggestions during the research work. I also would like to thank to my Master's Scrutiny Committee members for their valuable comments. I am grateful to my lab mates, Ashirbad Swain, D. Koteswara Rao and Benedict Thomas for their valuable helps.

After the completion of this Thesis, I experience a feeling of achievement and satisfaction. Looking into the past I realize how impossible it was for me to succeed on my own. I wish to express my deep gratitude to all those who extended their helping hands towards me in various ways during my tenure at NIT Rourkela.

I greatly appreciate and convey my heartfelt thanks to my colleagues 'flow of ideas, dear ones and all those who helped me in the completion of this work. I would like to thank my mother Kochurani Jose P for their love, sacrifice, and support. I wish to thank my brothers Jackson Jose and Jimson Jose for their encouragement, support, and endurance during the past few years.

**JEFRIN JOSE P.**

Roll No: - 612ME307

# ABSTRACT

The robotic manipulator is a device to carry out the various tasks according to the requirements without any human intervention. Vibration analysis of flexible manipulators has been an important area of research in order to model and control of such systems. In the present analysis, the Timoshenko beam theory based single and double link flexible manipulators made up of advanced composite material have been analyzed using finite element method. A three noded beam element has been implemented for modelling and analysis of the flexible composite manipulators under different input torques. The effects of hybridization of the different composite materials on the positions and residuals of the end effectors have also been studied. The input shaping has also been carried out in order to reduce the residual vibration of the end effector by adjusting the amplitude and time delay. The influences of the taper angles of the tapered flexible composite manipulators on the end effector movement and vibration have also been presented. The linear quadratic regulator control (LQR) scheme has been applied in order to further reduce the residual vibration of the end effector. Various results have been obtained based on the different analyses. The results reveal that the tapered hollow flexible composite manipulators give the better performances in terms of end effector positions and residual vibration. The obtained results based on the LQR control scheme show that residual vibration can be controlled without compromising the end effector movement.

# TABLE OF CONTENTS

# List of Figures

# List of Tables

# Chapter 1

## 1 Introduction

The rigid manipulators have high positional accuracy than flexible manipulators but the power required for attaining the positional accuracy are very high due to their high inertia. The flexible manipulator has low weight compared to rigid one. The manipulator made up of advanced composite materials have low weight, high specific stiffness and strength, and higher energy efficiency with better payload capacity. Hence it finds many applications. The improvement of the accuracy of a flexible open kinematic chain is a very emerging research problem. The advantage of flexible robotic arm fabricated with advanced composite material are increasingly being proposed, proved and developed in order to achieve high performance compared with heavy and rigid robotics arms. Due to the residual vibration, there is a possibility of failure of the flexible manipulator under the high payload situations. The control design of flexible manipulator must also take into account the presence of uncertainties in the model. The researchers are actively involved in order to reduce vibration and control of flexible manipulators. The control of manipulator mainly carried out by using two methods such as feed forward and feedback control techniques. The linear quadratic regulator (LQR) controller is a modern control technique which is designed in order to maximize the gain by minimizing the objective function or performance index. To materialize these, the following points are important.

i. To develop an efficient computational tool to simulate the behaviour/response of flexible composite manipulators subjected to loads considering any number of plies, orientations and materials structures. Finite element (FE) methods have already been extensively used for analysis and hence significant attention has been paid by researcher in recent times for development of efficient FE for analysis of such systems.
ii. To study the effects of hybrid composites on the responses of flexible composite manipulators in order to find more energy efficient material for robotic manipulators
iii. To study the responses of tapered flexible composite manipulators compared to conventional prismatic manipulators and
iv. To develop suitable control scheme which optimizes the controller gain so that most effective control could be achieved with minimum control input.

Robots are specially desirable for certain work functions because, unlike humans, they never become tired; they can sustain physical circumstances that are uncomfortable or even hazardous; they can work in airless circumstances; they do not get tired by repetition; and they cannot be diverted from the task at hand. The ease with which they can be programmed

and the accuracy with which they can carry out repetitive tasks leads to their wide spread use in industry. Moreover, increasing labour costs, as well as the capability of executing tasks which are impossible, difficult, or dangerous to humans are other motives for the increased use of robots in manufacturing lines.

Robotic manipulators are made by links joints to produce the kinematic chains. Joints are usually revolute (rotary) or prismatic (linear). A revolute joint is type of joint and permits relative rotation between two links. A prismatic joint permits a linear motion between two links. Every joint signifies the connection corresponding between two links. The robotic manipulator are classified into several criteria, such as their geometry, their intended application area, or way in which the joints are actuated, their power source, or kinematic structure, or techniques of control.

## 1.1 Materials for Robotic Manipulator

The manipulator is the device to carry out different task according to the requirement of the human without any direct contact. The manipulator are made up of different materials. The properties of a material will determine its suitability for a design. The materials choose depend mainly on the environment where they are used. Another criteria is the easy to machining and shaping requirements. Weight of the manipulator and desired mechanical properties are also important.

Woods are usually low cost and can be shaped by means of ordinary tools. Hard type woods are used for modelling the buildings. The balsa wood is usually used to create model of airplanes. Plastic component can be easily made into different shapes by moulding. The usual plastic moulding process involves molten plastic inserted under high pressure and temperature into specially made metal systems (such as core and cavity). For robotics, there are less use of plastic materials. Normally HDPE (High Density Poly Ethylene) is used for building the robot chasing. The HDPE plastic can mainly be selected because of its low cost, lightweight, high strength, and easy machinability. The plastic has low thermal conductivity so it cannot be used for high temperature applications. The deformation is also higher than the other materials, so it cannot be implemented in case of high payload situations.

For robots, the most common conventional materials are aluminium and steel. Aluminium is a softer in nature and hence it is easy to machining but steel is much stronger. In every case, robot bodies can be prepared using sheet, rod, bar, channel, and other shapes because of the natural strength of metals. Aluminium is resistant to corrosion as well as

lightweight. Most significantly, it is very easy to shape, cut, bend, and drill. The vibration of the robotic manipulator **is** increased by using the aluminium. The metal must be able to carry the weight of the batteries, motors and other parts without unnecessary bending or flexing. The main drawback of the steel based manipulators are normally rigid in nature and the weight of the manipulator is also more. The power consumption of the robots for movement will also rise when the high weight manipulators are not flexible in nature. Weight of the manipulators offer benefits such as higher speed, improved mobility, better energy efficiency, and higher payload-to-arm weight ratio. Light weight links are mainly implemented to effectively attain the criteria's of high speed and high acceleration placement. Although, light weight parts are more prone to vibrate due to the inertia forces, tip mass and external forces due to actuators.

By using the composite material manipulator one can get the combined properties of the two or more materials. Composite materials are classified into two board categories (such as particulate and fiber reinforced composites). In particulate composites, the particles have various shapes and size which are randomly dispersed in the matrix. Examples of particulate composites are lead particles in the copper alloy and aluminium particle in the polyurethane rubber. In fiber reinforced composite, major constituents are reinforced fiber, matrix coupling agent, coating and fillers. Advanced fibers are mainly the load carrying members while matrix keeps them proper location and correct orientation, and also acts the medium by which the load to transferred through the fibers by means of shear stress. Coupling agent and coating which are applied to the fiber to improve the wetting and bonding with the matrix.

Fiber is the most important constituent of a fiber reinforced composite materials. They are major volume fraction of the composite and can take only tensile load along it but if it used as a fiber reinforced composites, it can contribute the major part of the tensile, compressive, flexural, or the shear strength and stiffness of the FRP composites. According to the requirements of the applications, different type of fibers are used such as carbon fibers, glass fibers, boron fibers, aramid fibers and ceramic fibers. For the present study, Kevlar fiber and graphite fiber are used. Kevlar is the type of armide fiber. The advantage of the Kevlar is low density, high tensile strength and low cost. The main characteristics of the Kevlar are high specific strength and stiffness, vibration damping, resistance of damage, fatigue and stress ruptures. The graphite fiber is the type of carbon fiber. The benefits of graphite fibers

are low coefficient of thermal expansion, very high tensile strength-to-weight ratio, high fatigue strength and high tensile modulus to weight ratio.

The matrix is used as epoxy resin. Epoxy resin is used due to easy to process, excellent mechanical properties, and high hot and wet strength properties. The epoxy resin matrix also gives a better adhesion to reinforcing fiber than polyester resins.

The behaviour of the composite material is studied by two methods such as micromechanics and macro mechanics). In micromechanics which deal with the local failure, such as fiber, matrix and interface failures. The constituent material can be examined on a microscopic scale without changing their internal structure. In the macro mechanics, properties are considered along the length and perpendicular to the fiber directions. In the present analysis, the dynamics behaviour of the composite material is considered by macro mechanics.

## 1.2 Kinematic and Dynamic Analysis of Flexible Manipulator

Kinematics mean study the motion of object without concern of the forces or moments that cause the motion. Robot kinematic states the analytical study of the motion of robot. For kinematic analysis requires to find out the kinematic model for the robotic. For kinematics modelling of manipulators mainly used two dissimilar spaces i.e. Quaternion space and Cartesian space. The transformation between two Cartesian coordinate systems can be represented into a rotation and translation. The kinematic problems of robotic are solved by two methods such as forward and inverse kinematics. In forward (direct) kinematics, the position and orientation of the end point effector are calculated by means of group of joint angles where as in inverse kinematics, the joint angles are determined by means of position and orientation.

Robotic dynamics mean that the study deals with motion of the manipulator considering the force and moment which cause that motion. For controlling the position of the robot for required accuracy, it must know about the dynamic behaviour of the robots. For example, if little force exert on the manipulator and it will slowly respond and for more force exert, the manipulator will oscillate about its preferred position. The dynamic equation of motion can be derived by different methods. Euler-Lagrange equations, which define the development of a mechanical system subject to holonomic constraints. The dynamic problems of the robots are normally solved by three type of techniques such as experimental, analytical and numerical methods. Experimental method is more costly, time consuming and less

possibility to variation of system parameters. Analytical method is in rigorous one provide exact solution but hard to use complex problems. The Euler-Lagrangen equation may be derived from the principle of virtual work. For determining the Euler-Lagrangen equation, first has to form Lagrange of the system which is difference between kinetic and potential energy. The method is for evaluating the dynamics of robot manipulators well-known as the Newton-Euler formulation. In the Newton-Euler formulation consider each link of the manipulator in turn, and express the equations define its angular motion and its linear motion. Obviously, since each link is coupled to additional links, these equations which define each link carry coupling forces and torques that appear moreover in the equations that designate next links. The main disadvantages of the analytical methods are difficult to solve the complex problems.

Numerical methods have the improvement of the computing competences, and although they give approximate results, have enough accuracy for engineering purposes. The Runge-Kutta method is one of numerical methods for solving the equations. For a differential equation that define performance over time, the numerical method starts with the initial values of the variables, and then uses the equations to solve the alterations in these variables over a very short time period. In modelling of flexible manipulator are widely used numerical analysis methods viz. Finite Element Method (FEM), Assumed Mode Method (AMM) and Finite Difference Method (FDM).

## 1.3 Control of Flexible Manipulator

The state of the art in robot manipulator control is that manipulators are assumed to be rigid structures. Controllers that use joint variable feedback information, are designed based on that assumption. The flexible manipulator have structural flexibility as compared to the rigid link. Structural flexibility of the flexible manipulator is become significant. However, it is limit the performance of a control system when manipulator is large structure, manipulating on large payload, and/or operating at high speed.

Advanced motion control of robotic manipulators were studied by academic and industrial researchers since the beginning of the 1970's. The main approach for controlling an elastic manipulator is considered to be linear feedback in combination with nonlinear feed forward or feed-back linearization control. The control of robot manipulators can be described and classified in many ways e.g.

i. Type of drive system (direct drive or gear transmission)

ii. Type of model used (model-based such as rigid models, flexible joint models, or flexible link models) for the control
iii. Controlled variable (position, speed, compliance, or force)
iv. Motion type considered (high-speed continuous path tracking, low-speed continuous path tracking, point-to-point movement, tracking in contact with the environment, or regulation control)
v. Type of control law (linear/nonlinear, feedback/feed forward, static/dynamic, robust/ adaptive) and
vi. Type of measurements (actuator position, actuator speed, link position, link speed, link acceleration, link torque, tool position, tool speed, tool acceleration, tool force, or tool torque)

The different control techniques used for manipulator are position control, force control, and vision based control. The position control deals with motion control difficulties which contain of the tracking and disturbance rejection so it is difficult for finding the control inputs essential to monitor, or track, a chosen trajectory that to be scheduled for the manipulator. The torque control is also used for getting the accurate position control of the manipulator.

## 1.4 Organization of the Thesis

The present thesis has been organized as follows.

Chapter 1 discusses the brief introduction of the robotics, significance of the structural design of the flexible manipulator, importance of the material for robotic manipulators, vibration analysis and control technique used for the flexible composite manipulator, and outline of the thesis.

In order to understand the state of art in the broad field of modelling, analysis and vibration control of flexible composite manipulators a comprehensive literature review has been done and presented in chapter 2. Chapter 2 also includes the motivations from the exhaustive literature review and objectives of the present work.

Chapter 3 presents the detail of mathematical formulation of the flexible single and double-link manipulator using the developed three noded layered beam element based on the Timoshenko beam theory. The mathematical modelling involves governing equation, dynamic analysis, finite element formulation, state space representation, free vibration analysis, formulation of input shaping and LQR control techniques.

In Chapter 4, results of the flexible single and double links composite manipulators have been presented based on the formulations given in Chapter 3. This chapter also discusses the free vibration, dynamic analysis of flexible single and double-link composite manipulators by changing the different important parameters, and control of such manipulators.

Finally in Chapter 5, some important conclusions from the present work have been presented. Again scopes for the future extension of the present work have also been outlined in this chapter.

# Chapter 2

# 2 Literature Review

This chapter contains an exhaustive literature reviews in the broad fields of dynamic and control of flexible manipulator. Some of the important research works have been presented in the sub field of kinematic, dynamic and control of such manipulator systems. Firstly it is concentrated on the kinematic analysis of robotic manipulator. Then concentration is given to the literatures related on the dynamic analysis of manipulator. Finally, the focus of interest shifts to control techniques used for the said manipulator and motivation, and objectives based on the literature reviews has also been presented in the end of this chapter.

## 2.1 Kinematic Analysis of Robotic Manipulators

Kinematic analysis concerned with the motion of objects without reference to the force which causes the motion. It is important to know the position and orientation (geometric configuration) of a robot, along with velocities and accelerations of the robot components (links) in order to monitor and properly control the manipulator. There are numerous possible methods to use prismatic and revolute joints to build kinematic chains, in practice only a limited of these are usually used. In robotics, there are two kinematic tasks, first one direct (also forward) kinematics and second inverse kinematics. In direct kinematics finding the position and orientation of the end point effector by using group of joint angles but in case of inverse kinematics calculating the joint angles by using position and orientation.

Ataf et al. [1] presented the dynamic analysis of a flexible manipulator considering single link with a payload at the end of the manipulator. The analysis was done by means of tangential coordinate system (TCS) and the virtual link coordinate system (VLCS). The extended Hamilton's Principle was used for deriving the governing equation and found the maximum deflection at the distal end by considering TCS was much more than the maximum deflection at the center point of the VLCS for in the first mode shape. The TCS signifies the kinematics of the single link more accurate and in a real manner compared to the VLCS which carried out the condition that the deflection at the distal end is zero. Kumar et al. [2] presented a theoretical approach which gives the forward kinematics and inverse kinematics values but to find individual velocity, force, torque values of each link and joint was complicated. By using robot analyser it can easily identify velocity, acceleration graphs and their values regarding the joints and links and simulation of robot end effector can be done. Manjaree et al. [3] presented forward and inverse kinematic analysis of robotic manipulator with three degree-of-freedom (DOF) by moving in 3D spaces. Neuro-fuzzy intelligent technique viz. ANFIS was used. An example of triangle in three positions was used for comparisons. The comparison drawn on the methods show that the results obtained for inverse kinematics were

in reasonable agreement with one another though for some positions, the results differ. Al-Faiz and Saleh [4] presented an algorithm to find the inverse kinematics for a robotic manipulator with wrist offset. The proposed algorithm starts from finding the wrist point by vector computation, then compute the first three joint angles and after that compute the wrist angles by analytic solution. Eliot et al. [5] presented the design, construction and analysis of a five axes articulated robotic manipulator. The direct kinematic model was implemented in order to calculate the end effector's position and orientation.

Chang et al. [6] presented a modelling technique called "wheel-center modelling" for kinematics of a wheeled mobile robot that moves on irregular ground. The inverse kinematics solution for the lunar rover was used to control the motion of the rover. To model kinematically a six wheeled mobile robot by the "wheel-center modelling" technique was introduced in detail. Manjunath [7] studied a 5-axis stationary articulated robot arm with features the kinematic modelling which was used for doing an effective robotic manipulation job in its workspace. A 5-axes articulated robot was designed and a brief kinematic modelling was performed and using this kinematic model, the robot successfully performed the pick and place task in the workspace. Zarkandi and Esmaili [8] studied the forward position kinematics of a three (DOF) parallel manipulator with three identical limbs which may revolute-prismatic-spherical (RPS), and analysed it is three parametric equations used to represent the legs of the manipulator, a system of three nonlinear equations in three unknowns was attained. By using the Sylvester dialytic elimination method, the system of equations were reduced to a univariate polynomial of degree of eight and two quadratic equations. He et al. [9] presented a two-body mobile robot with a kind of modelling method that provides its kinematic structure constraints and analyses the direct kinematics and inverse kinematics. Considering the significance of superior problems in performing a complex task of the mobile robot, the results of inverse kinematics was identified using the geometric approach in particular specific conditions. The foremost contributions was to analyse the surpassing problems and rotating in different modes because the robot can alter the configuration actively. Results were revealed that the robot was a good capacity of surpassing problems actively. The rotating ability was analysed through many different ways and the result showed that the big difference of speeds and included angle will advantage to rotate.

## 2.2 Dynamic Analysis of Robotic Manipulator

A robotic manipulator is mainly a positioning device. To control the position it must identify the dynamic parameters of the robot in order to know how much force to utilize on it to reason it to move. The dynamic equations clearly define the relationship concerning force and motion. The equations of motion are significant to study in the design of robots, in simulation and animation of robot motion, and in the design of control systems. The dynamic equations can mainly be deduced using three methods which are classical methods, assumed modes method (AMM) and finite element method (FEM).

Based on the literature survey, some of the important work are related to the present work are listed here. The list is carefully chosen and related mostly to the present work done. Kalyoncu [10] presented a single link manipulator contains of a revolving prismatic joint and a sliding robot arm with a payload at the tip, investigations were carried out by studying the mathematical model and finding dynamic response of a flexible robot manipulator with rotational-prismatic joint. Flexible arm carrying an end-mass was modelled based on the Euler–Bernoulli beam. Here under the action of an external driving torque and an axial force, the tip end of the flexible robot manipulator traces a multi straight line path. Lagrange's equation used to find the governing equation of the flexible manipulator where effect of rotary inertia, axial shortening and gravitation was considered in the analysis. Hussein and Al-Robaiy [11] presented a modelling process of single link flexible manipulator. The equation of motion of the system for clamped and pinned boundary conditions were solved by finite element method (FEM). The nonlinear terms such as payload inertia and viscous friction factors were added to the model matrices. The model was presented in two forms, one in matrices form and the other in state space form. Tokhi and Mohamed [12] presented the performance evaluation and computational requirements of the FE method in the dynamic simulation of a flexible manipulator. A simulation of dynamic performance of a flexible single link manipulator was carried on the basis of precision and computational efficiency. It has been shown that by increasing the number of elements, better accuracy in the characterization of the system is attained with the FE method. However, processing time increased nonlinearly. Ahmad et al. [13] presented a dynamic analysis of single link manipulator including damping and hub inertia using finite element methods and addressed the effect of beam length on the system performance. The resonance modes of vibration of the system moved to lower frequencies and produces a slower response with increasing the length. Loudini et al. [14]

presented the planar single link flexible robot manipulator clamped at its actuated base and carrying a tip mass using modelled based on the Timoshenko beam theory (TBT). The effects of shear and rotary inertia of the flexible link cross-section were compensated by including the internal structural viscoelasticity effect (Kelvin-Voigt damping) and external viscous air damping. The Lagrangian approach combined with the assumed modes method was proposed to derive the dynamic model for the planar single link lightweight manipulator.

KhalilIbrahim et al. [15] presented the single link flexible arm with the development of efficient approach to dynamic modelling and mode analysis. The modelling of a single link flexible manipulator on the basis of the Euler-Bernoulli beam and Lagrange's equations of the motion were briefly discussed and accurate modes of the system were attained analytically. It was found a good agreement between the experimental and simulation results were dynamic model was suitable to describe the open loop response of a single flexible arm. Korayem et al. [16] presented the effect of the beam's length, shear deformation and different beam theories on the dynamic modelling of single link manipulator. At the first step, the Euler-Bernoulli beams theory (EBBT) was adopted. Next step the Timoshenko beam theory (TBT) was considered. Here, two types of dynamic models based on the Euler-Bernoulli and Timoshenko, were established and used to analyse the dynamic performance of the system. The results was showed that it is better to use (EBBT) for multi flexible link manipulators with longer length but if the links have short length it should use (TBT) for more accuracy. Oguamanam et al. [17] presented some important issues involved in the dynamic modelling of single link manipulators. These are the selection of reference frames, the determination of closed-form eigen functions expressions for use in the assumed mode method (AMM), and the role of geometric stiffening. It was observed that the choice of reference frames will affect the complexity of the resulting system equations of motion, but there are transformations that map one frame to the other. In determining the eigen functions, the role of tip-mass was treated in a more generalized form by using reference frames that permit a lucid reflection of the coordinates of the offset of the center of gravity of the tip mass from the point of attachment to the beam. Wang and Wei [18] modelled flexible single link robot manipulator modelled by considering moving slender prismatic beam. It was observed that the extending and contracting motions have destabilizing and stabilizing effects on the vibratory motions separately. The vibration of the system was analysed based on a Galerkin approximation with time-dependent basis functions.

Zohoor and Kakavand [19] considered a two-link flexible manipulator of a prescribed motion, the Timoshenko and Euler–Bernoulli beam models were considered. Using the Galerkin method, nonlinear equations of motion were solved. It was demonstrated that for two link manipulators, both theories provide good models and the results for both theories were very similar for the entire range of slenderness ratios. It was also known that for the high slenderness ratios, both theories act similarly. It is found that for two link planar manipulators with relatively high slenderness ratios there is a remarkable difference in models. It is obvious for high precision applications the Timoshenko model was recommended, and for low precision applications in low and medium ranges of speed, the Euler–Bernoulli model is suitable. It is also interesting that the joint torques in the entire range of slenderness ratios are the same. Gripp et al. [20] presented the modelling and identification of a two link manipulator with mechanical flexibility distributed along the links. The two link manipulator was modelled using the assumed mode method. The Lagrangian approach leads to explicit equations of motion. Actuators and sensors were also modelled in order to derive a complete and explicit model of the complete system. The theoretical model was simulated and compared to experimental results. Parametric identification successfully was fitted to the theoretical and experimental frequency response functions.

Chen [21] presented a dynamic model for multi-link planar flexible manipulators which contain an arbitrary number of flexible links. The elastic deformation of multi-link manipulator was modelled by means of the assumed mode method (AMM). Flexible links were modelled based on Euler-Bernoulli beams and ignoring the rotary inertia and shear deformation are thus ignored. Trapezoidal torques with changeable slopes but constant magnitude and period were applied to examine the dynamic behaviour of the links to the corresponding torques. Steeper torques tend to stimulate higher flexible deformations of the link. But the variance between the magnitudes of the flexible deformations was not very significant. The difficult as to which kind of driving torque stimulates the minimum flexible deformation was the best solution by inverse dynamics based on the computed torque method. Theodore and Ghosal [22] presented the axially translating flexible link manipulators with a prismatic joint modelled based on the Euler Bernoulli beam equation combined with the convective terms. To find a time-dependent frequency equation for the translating flexible beam based on clamped-mass boundary conditions, a novel method was presented to finding this time dependent frequency equation by considering a differential equation of the frequency

equation. A systematic modelling method was also presented for spatial multi-link flexible manipulators having both revolute and prismatic joints. The equation of motion was derived by employing assumed mode method and Lagrangian formulation.

Shaker and Ghosal [23] also presented nonlinear modelling of planar single and two link, flexible manipulators with rotary joints using finite element method (FEM) based approaches. The non-linear models, were derived from a non-linear strain-displacement relationship of the planar flexible manipulators with single and two revolute joints. The formulated FE mode method of modelling was compared with the conventional component mode method. The comparison of linear and nonlinear models. It has been cleared that nonlinear model can employ only if flexural rigidities of the links are low. Pratap and Reddy [24] presented the flexibility and dynamic analysis of flexible manipulator considering deflection. The distributed parameter method, was implemented to derive the generalized equation of motion of robot manipulator with flexible links. Elastic deformations of the flexible manipulator arms were found by using ANSYS-12.0 software package. Elastic compensation was introduced in the co-ordinates of robotic programming to acquire precise end-effectors path. A comparison of path trajectories and variation of torques were also studied after considering elastic compensation. Torby and Kimura [25] presented the revolute prismatic prismatic (RPP) model used to introduce 16 flexural (DOF), but the computer algorithm was such that an infinite amount of links can be treated. The prismatic links were considered as beams with moving boundary conditions, and the location of finite-element node points were not different relative to the link. They are compared with the eigenvalues attained for the same problem considering the assumed-mode method (AMM). The curves were very similar except for the higher natural frequencies found using the finite-element method. Al-Bedoor and Khulief [26] formulated a dynamic model of a translating and rotating beam by finite element method. The time dependent boundary condition obvious by the prismatic joint constraint were measured. In the FEM formulation the inertia coupling among the beam reference motion and local elastic deformation were considered. A transition element with variable stiffness was interfaced with the joint hub. These models have some benefits over the previously reported models as it avoids numerical problems because the nodal point belongs to a fixed finite element mesh.

## 2.3 Control Techniques used in Multi-Link Manipulators

The control of robotic manipulators has been an important field for study, development, and manufacturing. Industrial manipulators are mainly positioning and handling devices. Therefore, a suitable robot is only that is capable to control its motion and the interactive forces and torques between the manipulator and its location.

Tokhi et al. [27] presented a study into the improvement of an interactive and user friendly location for simulation and control of flexible single link manipulators using Simulink. A planar single link flexible manipulator was modelled and finite difference (FD) method was used in discretizing the governing dynamic equations of motion of the system. Open loop control strategies using bang-bang, Gaussian shaped and filtered command inputs were developed and implemented within the simulation environment and possible control strategies were presented and discussed. Yih [28] presented a modelling of single link flexible robot arm. The equation of motion of the system was solved by finite element method (FEM) where the clamped boundary conditions were considered and bang-bang torque was used to drive the system. Then the adaptive input shaper was presented. The adaptive input shaper was effective to the changes of dynamic response in the system. The amplitude and the time delay of the impulses were the parameters to the changes in the dynamic response of the system. Akyuz et al. [29] presented design and control of the single link joint manipulator. A cascade fuzzy logic controller (FLC) used to remove the vibration of link as well as trajectory tracking performance and also compared the performances of the cascade FLC with the PID controller, step input was applied to the system. Based on the comparison, the proposed FLC yield better result than the PID controller. It was also demonstrated the robustness of the controller, external disturbances and change in parameters such as link length and spring stiffness were employed. Mohamed and Tokhi [30] implemented the feed forward control strategies for vibration control of a single link manipulator by means of command shaping techniques based on the input shaping, low pass filter, band stop filter. The dynamic model of the flexible single link manipulator was determined by the finite element method. Significant drop in the system vibration was attained with these control strategies. From this analysis clears that low pass filter input has been revealed to achieve better performance than the band stop filter input. The processing time rising for an input shaping command is longer than required for the filtered input. Sa'id et al. [31] studied the dynamic modelling and step input tracking control of single flexible link. Two approaches to control were used for the

flexible link manipulator. The first one was a hybrid (i.e. PD and sliding mode) controller. Where, the augmented PD controller was used as a hub position control while the sliding mode control was used to damp out the vibration of tip position. The second control approach was to use a fuzzy based PI controller for control both of the hub angle and tip deflection. From the analysis, hybrid controller shows the better behaviour than the proposed fuzzy based PI controller for the single flexible link manipulator. Shaheed et al. [32] studied the open loop control configuration and used for vibration reduction of the flexible manipulator using genetic algorithm. Low pass and band stop filtered were developed and investigated in an open loop control configuration. It was revealed that better performance can attain in case of low-pass filtered input as compared to band-stop filtered torque input.

Subudhi and Morris [33] modelled and analysed the dynamics of a manipulator with multiple flexible links and flexible joint based on a combined Euler Lagrange formulation and assumed modes method (AMM). The control difficulties were resolved by considering a singularly perturbed model to design a reduced order controller, which was revealed to become stable the link and joint vibrations efficiently while retaining good tracking performance. Zebin and Alam [34] presented a theoretical study for the dynamic modelling, analysis and representation of a constrained two link flexible manipulator, by considering FE method. The final derived model of the system was simulated to study the dynamic response of the system. The end point vibration of a flexible manipulator has been reduced by adding of a Genetic Algorithm (GA) based fuzzy logic control strategy without compromising its speed of response. An uncoupled fuzzy logic controller method was also implemented with each controllers at the shoulder and the elbow link applying hub angle error and hub velocity feedback. Bottega et al. [35] presented tracking control model for a flexible single link manipulator by means of motor torque piezoelectric actuator. The Lagrange equation has been implemented to the dynamic modelling of the single link manipulator. Piezoelectric actuators and sensors were established to the system to control the high frequency vibration. Rigatos [36] developed the robust control approach for flexible-link robots that comprises sliding-mode control theory and kalman filtering. Sliding-mode control is a state feedback-based control approach which enables the flexible manipulator joints to track accurately.

Shan et al. [37] also presented feed forward approach based on input shaping implement to decrease vibration of the flexible system. In this research work, the modified input shaping (MIS) method was projected to develop better performance. The response of the manipulator

was compared in detail between the modified input shaping (MIS) method and the traditional input shaping (TIS) method. The MIS method is easier than the (TIS) method because the numerical optimization is avoidable in the design of the MIS shaper. However, to acquire a reasonable shaper with the TIS method, optimization is essential. Tang et al. [38] implemented a planar two link flexible manipulator to control the tip position based on neural network (NN) controller. The dynamic error was used to construct NN controller. The output redefinition approach was also used to derive the NN controller. Without the filtered tracking error, the offered NN controller has been still assurance the closed-loop system consistently asymptotically stable in addition to neural network weights bounded. To compare with the offered controller, Lewis's NN controller was also extended to the flexible link manipulator. Simulation response of a planar two link flexible manipulator revealed that the suggested NN controller decreases the vibration of the manipulator efficiently and also can make the tracking error converge to zero very rapidly. Kuo and Lin [39] presented a rotating thin flexural link with an entire control strategy which contains a design based model, controller design, and system output alteration for a distributed parameter system. The finite element modelling and the state space representation was presented successfully for control system analysis and computer simulation. It has been revealed, by directly tuning the system proportional gain, the rotating flexural link system can reach the desired damping ratio and the response has been attained that is exactly ten times faster than the first natural cantilever period of the system. Mansour and Kazi [40] proposed a single link flexible manipulator and vibration control by Modified Proportional-Integral- Derivative (MPID) control. To find the gain for optimal vibration control of the MPID controller a fuzzy logic tuning scheme was used. The recommended fuzzy logic scheme calculate an optimum vibration control gain that reduces the tip vibration for the end effector of the single link flexible manipulator. The main benefit of using fuzzy logic is the capacity to include the effect of varying the system configuration, environment constraint in addition to the PD control gains to obtain best tuned gain. Wang et al. [41] presented a new method to robust control of a multi-link flexible manipulator via regional pole assignment. A multi objective instantaneous awareness problem was presented to the controller design such that the controlled manipulator system, for all permissible parameter qualms in the operating space, instantaneously satisfies both the predetermined norm constraint on the transfer function from disturbance inputs to system outputs, and the predetermined circular pole constraint on the closed-loop system matrix.

## 2.4 Motivation

From the exhaustive literature review, the following important observations have been made.

i. A large number of research work available for dynamic analysis of flexible manipulator based on the Euler Bernoulli beam theory whereas very few works considered the Timoshenko beam theory.

ii. Most of the researchers analysed the manipulator made by conventional materials and only very few researchers have considered advanced composite for modelling and analysis.

iii. Most of the available research consider prismatic manipulators for modelling, analysis and control.

iv. PID control technique found to be focus on flexible single link manipulator and only very few research work considered the LQR control scheme

## 2.5 Objectives of Present Work

Keeping the above points in mind, the specific objectives of the present thesis have been laid down as

i. To model and analyse the single and flexible multi-link composite manipulators using the Timoshenko's beam theory based finite element method

ii. To study the influences of hybrid composites on the responses of flexible manipulators

iii. To study the responses of flexible composite manipulators under different input torques

iv. To analyse the flexible tapered solid as well as hollow composite manipulators in order to study the influences of taper angles on the responses of such manipulators

v. To incorporate the material damping based on the Rayleigh damping model so as to study the effects of damping on the responses of such manipulators

vi. To analyse and study the responses of such manipulators based on input shaping and

vii. To control the responses of such manipulators based on LQR control scheme.

# Chapter 3

# 3 Mathematical Formulation for Dynamic Analysis of Flexible Composite Manipulator

It is important initially to identify the flexible nature of the robots and formulate a mathematical model for the structure that accounts for connections with actuators and payload. Such a model can be implemented by considering partial differential equations (PDEs). Generally used method for solving a PDE signifying the dynamics of a manipulator, sometimes discussed to as the separation of variables method, and is to utilize a representation of the PDE attained through a simplification procedure, to a finite set of ordinary differential equations. Modelling of flexible manipulator can be derived by different approaches. The assumed mode method, singular perturbation, frequency domain, finite difference (FD) and finite element (FE) method are the various approaches to solving the (PDE)s expressing the dynamic properties of a flexible manipulator.

The dynamic equation of the manipulator has been derived normally by Hamiltonian equation. For modelling of manipulator is based on two beam theories. First one is the Euler Bernoulli's theory (EBT), in this theory mostly used for long or slender beams. In EBT shear deformation and rotary inertia effects are ignored. Second one is the Timoshenko beam theory (TBT), in this PDE based model is preferred because it is more accurate in calculating the beam's response compare to the Euler–Bernoulli (EB) beam. The TBT accounts for both the effect of rotary inertia and shear deformation.

In the present study the dynamic analysis of different links are carried out. The dynamic model of a physical structure (including rigid robotic manipulators) is obtainable by using Lagrange's equation. For robotic manipulators, the Lagrangian technique is simplified by first formulating certain (generalized) inertia matrices. This approach can be combined with the FE method to model the flexible links of robotic manipulators. The flexible link is considered as an assembly of a finite number of small elements. The elements are supposed connected at certain points, well-known as nodes. For each finite element, the scalar kinetic energy and potential energy functions are expressed as functions of the generalized coordinates. The dynamic model is obtained by applying Lagrange's equations. The element size is reduced, by increasing the number of elements, the general solution of the system equations can be made to converge to the exact solution as accurately as desired.

## 3.1 The Single Link Flexible Manipulator System

The flexible composite manipulator system is modelled as a clamped-free flexible beam with a mass at the hub which can bend freely in the horizontal plane but is stiff in vertical bending and torsion. The length of the manipulator is assumed to be constant and shear deformation as well as rotary inertia are also considered. The schematic representation of the flexible manipulators is shown in Fig 3.1 The payload mass is $M_p$ and input torque $\tau(t)$ is applied at the hub of the manipulator by an actuator motor. The angular displacement of the manipulator is denoted by $\theta_1(t)$. For an angular displacement $\theta_1$ and an elastic deflection $w$, the total displacement $y(x, t)$ of a point along the manipulator at a distance $x$ from the hub can be described as a function of both the rigid-body motion $\theta_1(t)$ and elastic deflection $w(x, t)$.

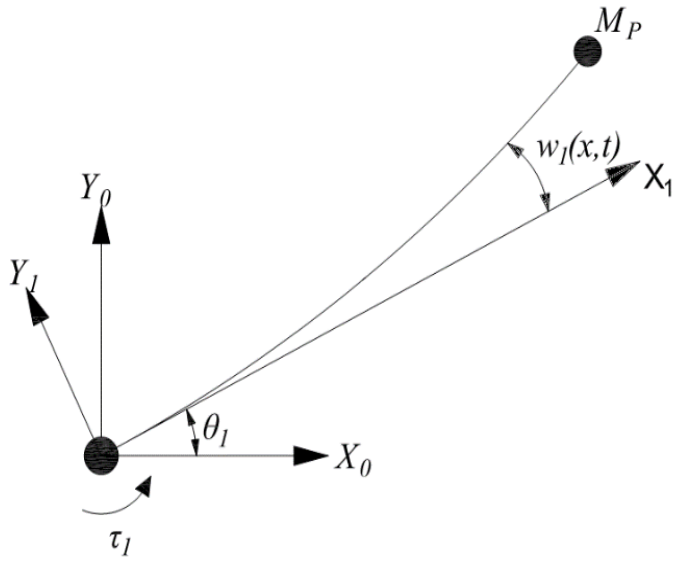


**Fig. 3.1 Schematic representation of the flexible manipulator system**

For an angular displacement $\theta_1$ and an elastic deflection $w$, the total (net) displacement $y(x, t)$ of a point along the manipulator at a distance $x$ from the hub can be described as a function of both the rigid-body motion $\theta(t)$ and elastic deflection $w(x, t)$ measured from the line OX.

$$y(x,t) = x\,\theta(t) + w(x,t) \tag{3.1}$$

To obtain equations of motion of the manipulator, the associated energies have to be obtained. These include the kinetic, potential and dissipated energies.

## 3.2 Various Energies Associated with the System

The energies associated with the system include the kinetic, potential and dissipated energy. These are considered for the SLFM in this section. As the contribution of the rotational moment of inertia is neglected, the kinetic energy of the system can be written as

$$E_k = E_h + E_l + E_{MP} \tag{3.2}$$

where

$$E_h = \frac{1}{2} I_h \dot{\theta}^2(t) \tag{3.3}$$

$$E_l = \frac{1}{2}\int_0^l \rho A \left\{ \left( \frac{\partial w(x,t)}{\partial t} + x\dot{\theta}(t) \right)^2 + \left[ \dot{\theta}(t)\omega(l,t) \right]^2 \right\} dx \tag{3.4}$$

$$E_{MP} = \frac{1}{2} M_p \left\{ \left[ \left( \frac{\partial w(x,t)}{\partial t} + x\dot{\theta}(t) \right)_{x=l} \right]^2 + [\dot{\theta}(t)\omega(l,t)]^2 \right\} + \frac{1}{2} I_p \left\{ \left[ \dot{\theta}(t) + \frac{\partial}{\partial t} \left( \frac{\partial \omega(x,t)}{\partial x}\bigg|_{x=l} \right) \right]^2 \right\} \tag{3.5}$$

Note in the above equation where $E_h$, $E_l$, $E_{MP}$ are the kinetic energies associated to the rigid hub, the flexible link, and the payload respectively. Moreover, note that only small elastic deflection and small angular velocity are considered.

## 3.3 The Dynamic Equations of Motion

The non-conservative work for the input torque τ can be written as

$$W = \tau\theta \tag{3.6}$$

To obtain the equations of motion of the manipulator, the Extended Hamilton's principle described by

$$\int_{t1}^{t2} (\delta L + \delta W) dt = 0 \tag{3.7}$$

can be used, subject to $\delta\theta$ and $\delta u \neq 0$ at $t_1$ to $t_2$, where, $t_1$ and $t_2$ are two arbitrary times, and $L = E_K - E_P$ is the system Lagrangian. $\delta W$ represents the virtual work, $\delta\theta$ represents a virtual rotation and $\delta u$ represents a virtual elastic displacement.

$$\delta \int_{t_2}^{t_1} \left( E_K - E_p + W \right) dt = 0 \tag{3.8}$$

For the two link manipulator the dynamic equation has been derived same as SLFM. The various energies associated with the two link manipulator are the sum of the energies of first link and second links. The dynamic equation of link 1 and link 2 are expressed as

The Lagrangian of link 1 can be derived as followed

$$\widehat{L}_1 = E_{K_1} - E_{P_1} \tag{3.9}$$

The Lagrangian of link 2 can be derived as followed

$$\widehat{L}_2 = E_{K_2} - E_{P_2} \tag{3.10}$$

Where the $E_{K_1}$, $E_{P_1}$ and. $E_{K_2}$, $E_{P_2}$ are the total kinetic energy and total potential energy of link 1 and 2 respectively. Now the total Lagrangian for both link can be given as

$$\widehat{L} = \widehat{L}_1 + \widehat{L}_2 \tag{3.11}$$

The Extended Hamilton's principle can be used to obtain the equations of motion of the double link manipulator.

## 3.4 Mathematical Modelling of Composite Beam based on the Timoshenko Beam Theory

The Fig.3.2 represents the configuration of the Timoshenko beam where $\beta_x$ is the Euler's angle which represents the rotation of the cross-section about an axis (refer Fig.3.2), which is mutually perpendicular to both *x* and *z* axes and assumed to be small compared to unity. Hence the kinetic energy of beam of length '*L*' is represented as

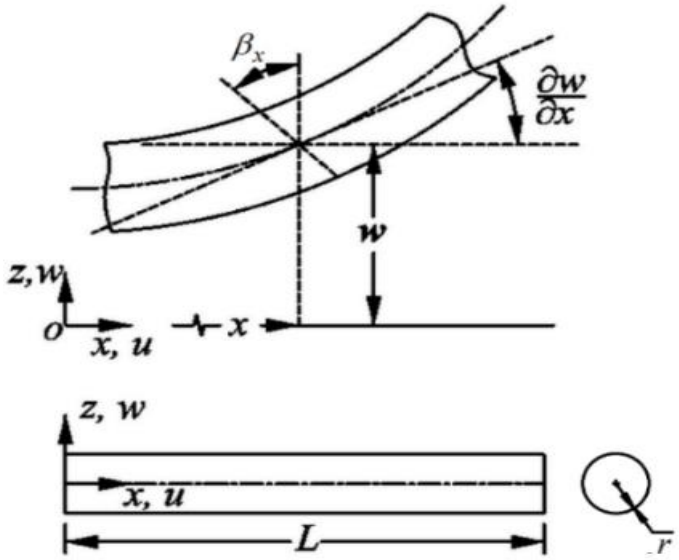


**Fig. 3.2 Deformed beam**

$$T = \frac{1}{2}\int_0^L \left( I_m \dot{w}^2 + I_d \dot{\beta}_x^{\,2} \right) dx \tag{3.12}$$

Where $I_m$ is to the mass intensity and denotes mass per unit length of the beam and $I_d$ diametrical mass moment of inertia of the cross-section of interest with inner and outer diameter $r_i$ and $r_o$ respectively. By taking the first variation in the kinetic energy gives

$$\delta T = \int_0^L \left\{ I_m \dot{w} \frac{\partial \delta w}{\partial t} + I_d \dot{\beta}_x \frac{\partial \delta \beta_x}{\partial t} \right\} dx \tag{3.13}$$

The second step is derive the expression of potential energy for which the displacement fields are needed and hence can be assumed to be

$$u_x(x,z,t) = z\beta_x(x,t)$$
$$u_z(x,z,t) = w(x,t) \tag{3.14}$$

where $u_x$ and $u_z$ are the flexural displacements of any point on the cross-section of interest along $x$ and $z$ direction respectively which are axes of coordinate system with origin at the centre of cross-section such that $x$ and $z$ remains parallel to inertial reference frame $X$ and $Z$ respectively. $u$ and $w$ represent flexural displacements of any point on reference exes of the beam. Linear elastic theory is applied to get the linear strain displacement relationship as

$$\varepsilon_{xx} = z\frac{\partial\beta_x}{\partial x}, \varepsilon_{xz} = \frac{1}{2}\left(\beta_x + \frac{\partial w}{\partial x}\right), \varepsilon_{yy} = \varepsilon_{zz} = \varepsilon_{yz} = \varepsilon_{xy} = 0 \tag{3.15}$$

The polar coordinate system (*x, r, θ*) is used for the convenience. Then the strain displacement relationship would results [43]

$$\begin{Bmatrix} \varepsilon_{xx} \\ \varepsilon_{x\theta} \\ \varepsilon_{xr} \end{Bmatrix} = \begin{bmatrix} 1 & 0 & 0 \\ 0 & -n & m \\ 0 & m & n \end{bmatrix} \begin{Bmatrix} \varepsilon_{xx} \\ \varepsilon_{xy} \\ \varepsilon_{zx} \end{Bmatrix} \tag{3.16}$$

where $m = \cos\theta$ and $n = \sin\theta$. Taking $z = r\sin\theta$, the strain displacement relation in terms of displacement variable would yield

$$\varepsilon_{xx} = r\sin\theta\frac{\partial\beta_x}{\partial x}, \varepsilon_{x\theta} = \frac{1}{2}\left(\beta_x + \frac{\partial w}{\partial x}\right)\cos\theta$$
$$\varepsilon_{xr} = \frac{1}{2}\left(\beta_x + \frac{\partial w}{\partial x}\right)\sin\theta, \varepsilon_{rr} = \varepsilon_{\theta\theta} = \varepsilon_{r\theta} = 0 \tag{3.17}$$

Hence the stress and strain expressed as

$$\begin{Bmatrix} \sigma_{xx} \\ \tau_{x\theta} \\ \tau_{xr} \end{Bmatrix} = \begin{bmatrix} \bar{Q}_{11} & k_s\bar{Q}_{16} & 0 \\ k_s\bar{Q}_{16} & k_s\bar{Q}_{66} & 0 \\ 0 & 0 & k_s\bar{Q}_{55} \end{bmatrix} \begin{Bmatrix} \varepsilon_{xx} \\ \gamma_{x\theta} \\ \gamma_{xr} \end{Bmatrix} \tag{3.18}$$

where $k_s$ is the shear correction factor. Hence the strain energy expressed as

$$U_s = \frac{1}{2}\int_V \{\sigma\}^T \{\varepsilon\} dV = \frac{1}{2}\int_V \left(\sigma_{xx}\varepsilon_{xx} + 2\tau_{xr}\varepsilon_{xr} + 2\tau_{x\theta}\varepsilon_{x\theta}\right)dV \tag{3.19}$$

By taking the first variation in the strain energy gives

$$\delta U = \int_V \left(\sigma_{xx}\delta\varepsilon_{xx} + 2\tau_{xr}\delta\varepsilon_{xr} + 2\tau_{x\theta}\delta\varepsilon_{x\theta}\right)dV =$$
$$= \int_V \left\{\sigma_{xx} r\sin\theta\frac{\partial\delta\beta_x}{\partial x} + \tau_{xr}\left(\delta\beta_x + \frac{\partial\delta w}{\partial x}\right)\sin\theta + \tau_{x\theta}\left(\delta\beta_x + \frac{\partial\delta w}{\partial x}\right)\cos\theta\right\}dV \tag{3.20}$$

$$\Rightarrow \delta U = \int_V \left\{ \sigma_{xx} r \sin\theta \frac{\partial \delta\beta_x}{\partial x} + \left(\tau_{xr} \sin\theta + \tau_{x\theta} \cos\theta\right)\left( \delta\beta_x + \frac{\partial \delta w}{\partial x} \right) \right\} dV \tag{3.21}$$

The stress resultants $N_x$, $Q_{xr}$, $Q_{x\theta}$ and stress couple $M_y$ are defined as

$$M = \int_A \sigma_{xx} r \sin\theta dA; Q_{xr} = \int_A \tau_{xr} \sin\theta dA; Q_{x\theta} = \int_A \tau_{x\theta} \cos\theta dA \tag{3.22}$$

The first variation of potential energy again can be written as

$$\delta U = \int_V \left\{ \sigma_{xx} M_y \frac{\partial \delta\beta_x}{\partial x} + \left(Q_{xr} + Q_{x\theta}\right)\left( \delta\beta_x + \frac{\partial \delta w}{\partial x} \right) \right\} dV \tag{3.23}$$

The stress resultants can be written as

$$M = D_{11} \frac{\partial \beta_x}{\partial x}; Q_{xr} = k_s A_{55} \left( \beta_x + \frac{\partial w}{\partial x} \right); Q_{x\theta} = k_s A_{66} \left( \beta_x + \frac{\partial w}{\partial x} \right) \tag{3.24}$$

The third step is to find the equation of motion of the system. Hamilton's principle is applied as follows

$$\int_{t_1}^{t_2} (\delta T - \delta U) dt = 0 \tag{3.25}$$

So the equation of motion can be written as

$$\begin{aligned} &\delta w : I_m \frac{\partial^2 w}{\partial t^2} + k_s \left(A_{55} + A_{66}\right)\left( \frac{\partial \beta_x}{\partial x} - \frac{\partial w}{\partial x} \right) = 0 \\ &\delta \beta_x : I_d \frac{\partial^2 \beta_x}{\partial t^2} - D_{11} \frac{\partial^2 \beta_x}{\partial x^2} - k_s \left(A_{55} + A_{66}\right)\left( \frac{\partial w}{\partial x} - \beta_x \right) = 0 \end{aligned} \tag{3.26}$$

Applying the value of stress resultants in Eq. (3.26), will result

$$\begin{aligned} &\delta w : I_m \frac{\partial^2 w}{\partial t^2} + k_s \left(A_{55} + A_{66}\right)\left( \frac{\partial \beta_x}{\partial x} - \frac{\partial w}{\partial x} \right) = 0 \\ &\delta \beta_x : I_d \frac{\partial^2 \beta_x}{\partial t^2} - D_{11} \frac{\partial^2 \beta_x}{\partial x^2} - k_s \left(A_{55} + A_{66}\right)\left( \frac{\partial w}{\partial x} - \beta_x \right) = 0 \end{aligned} \tag{3.27}$$

The terms $A_{55}$, $A_{66}$, $D_{11}$, $I_m$ and $I_d$ of Eq. (3.26) for $n$ number of composite plies are given as follows

$$\begin{aligned} &A_{55} = \frac{\pi}{2} \sum_{i=1}^{n} \bar{Q}_{55i} (r_{i+1}^2 - r_i^2) \ , A_{66} = \frac{\pi}{2} \sum_{i=1}^{n} \bar{Q}_{66i} (r_{i+1}^2 - r_i^2) \ , D_{11} = \frac{\pi}{4} \sum_{i=1}^{n} \bar{Q}_{11i} (r_{i+1}^4 - r_i^4), \\ &I_m = \pi \sum_{i=1}^{n} \rho \left(r_{i+1}^2 - r_i^2\right), I_d = \frac{\pi}{4} \sum_{i=1}^{n} \rho \left(r_o^4 - r_i^4\right); \ \ \bar{Q} = Q(\alpha, \delta) \\ &\alpha = \text{Effective taper angle}, \delta = \text{ply orientation} \end{aligned} \tag{3.28}$$

## 3.5 Finite Element (FE) Formulation of the Flexible Composite Manipulators

FE analysis aim is to find out the field variable (displacements) at nodal points by approximate analysis. In the present FE model, the three-nodded one-dimensional line elements are considered, each node having two degree of freedom (DOF) as shown in Fig.3.3. The Lagrange's interpolation functions are used to approximate the displacement fields of flexible beam. The element's nodal DOF at each node is . Now displacement field variable can be represented as,

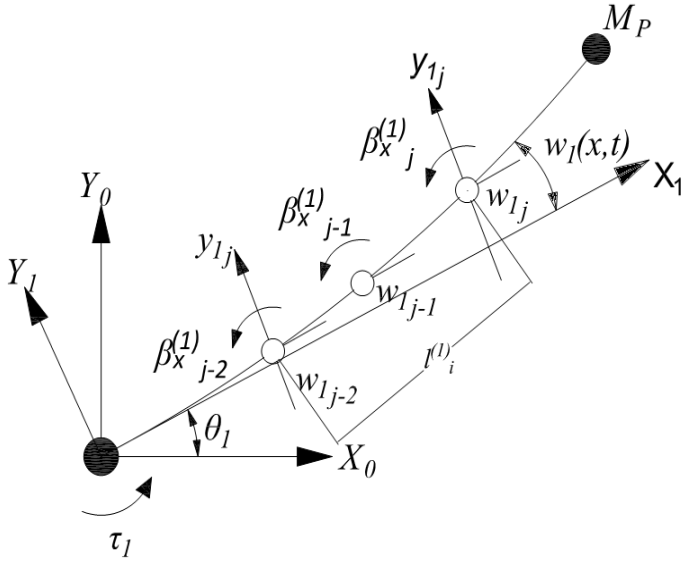


**Fig. 3.3 FE model of flexible single link manipulator**

$$w=\sum_{k=1}^{n} w^k(t)\phi_k(\xi),\ \beta_x=\sum_{k=1}^{n}\beta_x^k(t)\phi_k(\xi) \tag{3.29}$$

For three nodded element, the Lagrange's shape functions or Interpolating functions can be expressed as

$$\phi_1(\xi)=-\frac{1}{2}\xi(1-\xi);\ \ \phi_2(\xi)=1-\xi^2;\phi_3(\xi)=\frac{1}{2}\xi(1+\xi) \tag{3.30}$$

So the displacement field can be written as $w(x,t)=N_a(x)Q_a(t)$, Where $N_a(x)$ and $Q_a(t)$ represent the shape function and nodal displacement respectively. Hence, the total displacement can be obtained as $y(x,t)=N(x)q(t)$

Where

$$q(t) = [\theta_1(t) \quad Q_a(t)] \tag{3.31}$$

$$N_a(x) = [\phi_1(x) \quad \phi_2(x) \quad \phi_3(x)],$$
$$Q_a(t) = [w_{n-2} \quad w_{n-1} \quad w_n \ldots \quad (\beta_x)_{n-2} \quad (\beta_x)_{n-1} \quad (\beta_x)_n]^T \tag{3.32}$$

After putting the displacement field variables and shape function expressions into governing equations, the equation of motion for an element can be written as,

$$[M_e]\{\ddot{q}\} + [K_e]\{q\} = \{F_e\} \tag{3.33}$$

Where, $[M_e], [K_e], \{F_e\}$ are the elemental mass, stiffness and force vector respectively. The elemental stiffness and mass matrix can be determined as follows.

$$[K^e] = \begin{bmatrix} 0 & 0 & 0 \\ 0 & [K_w]_{3\times3} & \left[K_{w_{\beta_x}}\right]_{3\times3} \\ 0 & \left[K_{w\beta_x}\right]^T_{3\times3} & \left[K_{\beta_x}\right]_{3\times3} \end{bmatrix}; [K_w] = k_s(A_{55} + A_{66})\int_0^1 [N_w']^T [N_w'] d\xi \tag{3.34}$$

$$\left.\begin{aligned} \left[K_{w_{\beta_x}}\right] &= -k_s(A_{55} + A_{66})\int_0^1 \left[N_{\beta_x}\right]^T [N_w'] d\xi \\ [K_{\beta_x}] &= \left[\left[\frac{1}{L} D_{11}\int_0^1 [N_{\beta_x}']^T [N_{\beta_x}'] d\xi\right] + \left[k_s(A_{55} + A_{66})\int_0^1 \left[N_{\beta_x}\right]^T \left[N_{\beta_x}\right] d\xi\right]\right] \end{aligned}\right\} \tag{3.35}$$

$$\left.\begin{aligned} [M^e] &= \begin{bmatrix} M_{\theta\theta} & M_{w\theta} \\ M_{\theta w} & M_{ww} \end{bmatrix}, M_{ww} = \begin{bmatrix} M_{w_{3\times3}} & 0_{3\times3} \\ 0_{3\times3} & M_{\beta_{3\times3}} \end{bmatrix} \\ [M_w] &= \mathrm{I_m}\int_0^1 [N_w]^T [N_w] d\xi, \; [M_\beta] = \mathrm{I}_d \int_0^1 [N_\beta]^T [N_\beta] d\xi \end{aligned}\right\} \tag{3.36}$$

Where $K_w$ and $K_{\beta x}$ are the stiffness corresponding to axial displacement degree of freedom and rotational degree of freedom respectively. $K_{w\beta x}$ is the stiffness corresponding to coupling between displacement and rotational degree of freedom. $L$ is the length of the element and $M_{ww}$ is associated with the elastic degree of freedom (residual motion), $M_{w\theta}$ representing the coupling between these elastic degree of freedom and hub angle $\theta$ and $M_{\theta\theta}$ is associated with the inertia of the system about the motor axis. After assembling all elemental matrices and considering the Rayleigh damping model, the equation of motion of the flexible composite manipulator can be written as

$$[M]\{\ddot{\tilde{q}}\}+[C]\{\dot{\tilde{q}}\}+[K]\{\tilde{q}\}=\{F\} \tag{3.37}$$

Where $[M]$ is the global mass matrix, $[C]$ is the global damping matrix, $[K]$ is the global stiffness matrix. The force vector for flexible manipulator is taken as $F(t)=[\tau(t) \quad 0 \quad ... \quad 0]$ where $\tau(t)$ is the applied torque at the hub. The equation of motion for free vibration analysis can be written as

$$[M]\{\ddot{\tilde{q}}\}+[K]\{\tilde{q}\}=0 \tag{3.38}$$

The damping matrix (C) can be obtained as where $C_{ww}$ denote the sub-matrix associated with the damping of flexible manipulators. The matrix $C_{ww}$ is obtained based on the Rayleigh damping model as follows:

$$C_{ww}=\alpha M_{ww}+\beta K_{ww} \quad \text{Where} \quad \alpha=\frac{2f_1f_2(\xi_1f_2-\xi_2f_1)}{f_2^2-f_1^2} \qquad \beta=\frac{2(\xi_2f_2-\xi_1f_1)}{f_2^2-f_1^2} \tag{3.39}$$

Where $\xi_1, \xi_1$, $f_1$ and $f_2$ representing the damping ratios and natural frequencies of first and second modes respectively.

For the two link manipulator the finite element formulation can be derived same as SLFM.

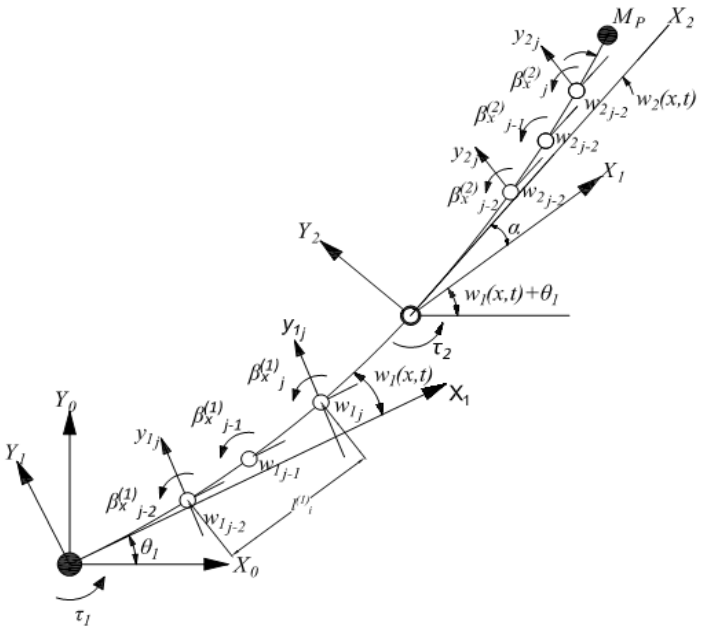


**Fig. 3.4 Finite element model with two link manipulator**

The Fig.3.4 shows the two links are connected together by serial manner. The total displacement of the two link flexible manipulator as same as the previous one. The Fig.3.4 describe the inertial systems of co-ordinates and the corresponding degree of freedom of the

finite element. The nodal displacement of the two link manipulator contain deformation of first and second link can be written as.

$$Q(t) = \left[\theta \;\; Q_{a_1} \;\; \alpha \;\; Q_{a_2}\right] \tag{3.40}$$

$$Q_{a_1} = [\, w_{1_{n-2}} \;\; w_{1_{n-1}} \;\; w_{1_n} \;\; \beta_{1_{n-2}} \;\; \beta_{1_{n-1}} \;\; \beta_{1_n}\,]; \quad Q_{a_2} = [\, w_{2_{n-2}} \;\; w_{2_{n-1}} \;\; w_{2_n} \;\; \beta_{2_{n-2}} \;\; \beta_{2_{n-1}} \;\; \beta_{2_n}\,] \tag{3.41}$$

The shape function are used for two link manipulator as same as previous one. The equation of motion of free vibration analysis is describe in the Eq. (3.38) where $[M]$ is the global mass matrix, $[C]$ is the global damping matrix, $[K]$ is the global stiffness matrix of the double link manipulator and.

The elemental mass matrix for the first and second link can be determined as.

$$\left[M_1^{\,e}\right] = \begin{bmatrix} M_{\theta\theta} & M_{w\theta} \\ M_{\theta w} & M_{ww} \end{bmatrix} \qquad \left[M_2^{\,e}\right] = \begin{bmatrix} M_{\alpha\alpha} & M_{w\alpha} \\ M_{\alpha w} & M_{ww} \end{bmatrix} \tag{3.42}$$

Where $M_{ww}$ is associated with the elastic degree of freedom (residual motion) is as same as the single link manipulator. After assembling all elemental matrices and considering the Rayleigh damping model, the equation of motion of the flexible composite double link manipulators can be written as

$$[M] = \begin{bmatrix} M_1 & 0 \\ 0 & M_2 \end{bmatrix}, \quad [K] = \begin{bmatrix} K_1 & 0 \\ 0 & K_2 \end{bmatrix} \tag{3.43}$$

## 3.6 State Space Representation

The second order matrix differential equation i.e. Eq. (3.37) can be represented in a state-space form

$$\dot{X} = AX + Bu \;;$$
$$y = CX \tag{3.44}$$

Where $\quad A = \begin{bmatrix} 0 & \mathrm{I} \\ -M^{-1}K & -M^{-1}C \end{bmatrix}; \; B = \begin{bmatrix} 0 \\ M^{-1} \end{bmatrix},$

$u = [\tau \quad 0 \quad ... \quad 0]$ and the state vector $X = [\theta \quad w \quad ... \quad \beta ... \quad \dot{\theta} \quad \dot{w} \quad ... \quad \dot{\beta} ...]^T$

## 3.7 Design of Input Shaper

The input shaping is done by adjusting the time delay and amplitude of the impulse response. The parameters used for the study are natural frequencies and damping ratio of the manipulator. The impulse response of the system can be obtained as

$$y(t) = \frac{A_{is}\,\omega}{\sqrt{1-\xi_d{}^2}} e^{-\xi_d\,\omega(t-t_0)} \sin\left(\omega\sqrt{1-\xi_d{}^2}\,(t-t_0)\right) \tag{3.45}$$

Where $A_{is}$ is the amplitude of the impulse, $t_0$ is the time of the impulse, $\omega$ is the natural frequency of the system and $\xi_d$ is the damping ratio of the system. The impulse response is found out by superposition of the impulse responses. For the $N$ impulses with $\omega_d = \omega\,(1-\xi_d{}^2)^{1/2}$, the impulse response can be expressed as

$$y(t) = M_{is} \sin\left(\omega_d\, t + \beta\right) \quad \text{Where} \quad M_{is} = \sqrt{\left(\sum_{i=1}^{N} B_i \cos\phi_i\right)^2 + \left(\sum_{i=1}^{N} B_i \sin\phi_i\right)^2}$$

$$B_i = \frac{A_i\,\omega}{\sqrt{1-\xi_d{}^2}} e^{-\xi_d\,\omega(t-t_0)} \quad \textit{and} \quad \phi_i = \omega_d\, t_i \tag{3.46}$$

Where the $A_i$ and the $t_i$ are the amplitude and time of the impulse. The residual vibration of the single mode amplitude of the impulse response is obtained as the time of the last impulse i.e. $t = t_N$ as

$$V = \sqrt{V_1^2 + V_2^2} \quad \text{Where} \quad V_1 = \sum_{i=1}^{N} \frac{A_i\,\omega_n}{\sqrt{1-\xi_d{}^2}} e^{-\xi_d\,\omega_n(t_N - t_i)} \cos\left(\omega_d\, t_i\right)$$

$$V_2 = \sum_{i=1}^{N} \frac{A_i\,\omega_n}{\sqrt{1-\xi_d{}^2}} e^{-\xi_d\,\omega_n(t_N - t_i)} \sin\left(\omega_d\, t_i\right) \tag{3.47}$$

To attain the zero vibration (ZV), the $V(\omega,\xi_d)$ is set to zero. A constraint must be applied to make certain that the shaped command creates the same rigid body movement as the unshaped command. To fulfil this requirement, the addition of the impulse amplitude must be one. For reducing the response lag, the first impulse is selected at time $t_i = 0$. So the $V_1$ and $V_2$ in the Eq. (3.47) is set to zero. By solving for two impulse sequences, the ZV shaper are obtained as:

$$t_1 = 0;\ t_2 = \frac{\pi}{\omega_d};\ A_1 = \frac{1}{1+2K^*+K^{*2}};\ A_2 = \frac{2K^*}{1+2K^*+K^{*2}} \tag{3.48}$$

To achieve the robustness of the input shaping process, an added constraint is utilized to design the input shaper. The derivative of the residual vibration with respect to the natural frequency is equal to zero. By setting the derivative to zero is same to producing small changes in vibration with corresponding changes in the natural frequency. By solving the three impulse sequences, the zero vibration derivative (ZVD) are obtained as:

$$t_1 = 0;\ t_2 = \omega_d\ ;\ t_3 = 2t_2\ ; A_1 = \frac{1}{1+2K^* + K^{*2}};\ A_2 = \frac{2K^*}{1+2K^* + K^{*2}};\ A_3 = \frac{K^{*2}}{1+2K^* + K^{*2}} \tag{3.49}$$

Where $K^* = e^{\frac{\pi\xi_d}{\sqrt{1-\xi_d{}^2}}}$ the vibration reduction was accomplished by convolving any desired system input with impulse sequences. This modified shaped input that drives the system to a desired location without vibration.

## 3.8 LQR Controller for Flexible Manipulator

Linear quadratic regulator (LQR) optimal control theory has been used to determine the control gains.

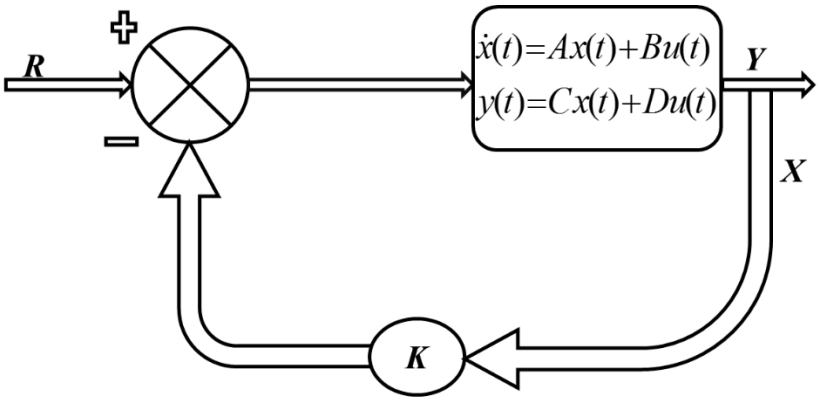


**Fig. 3.5 General robot feedback controller structure.**

A general feedback controller structure is illustrated in Fig.3.5. In this, the feedback control system has been designed to minimize a cost function or a performance index, which is proportional to the required measure of the system's response. The cost function (i.e. total energy of the system such as potential, kinetic and electrical energies) used in the present case is given by

$$J = \int_0^\infty (X^T Q X + u^T R u)\, dt \tag{3.50}$$

Where $u$ and $X$ are input and output vectors respectively, and [$Q$] and [$R$] are the semi-positive-definite and positive-definite weighting matrices on the outputs or states and control inputs, respectively. The steady-state matrix Ricatti equation can be written as

$$[A]^T[\mathrm{S}] + [\mathrm{S}][A] - [\mathrm{S}][B][R]^{-1}[B]^T[\mathrm{S}] + [Q] = 0 \tag{3.51}$$

The Eq. (3.51) can be obtained by forming an unconstrained optimization using Eq. (3.44) and Eq. (3.50). After solving the Ricaati equation using Potter's method, optimal gain can be written as

$$[G_c] = [R]^{-1}[B]^T[\mathrm{S}] \tag{3.52}$$

where [S] is solution of the Ricatti equation which is symmetric and positive definite matrix. Considering full state feedback, the control input to the hub can be determined as

$$\{\phi_a\} = -[G_c]\{X\} \tag{3.53}$$

Weighting matrices [Q] and [R] are important components of LQR optimization process. The compositions of [Q] and [R] elements influence the system's performance. The [Q] and [R] matrices could be determined considering weighted energy of the system as follows

$$[Q] = \begin{bmatrix} \alpha_2[\psi]^T[K][\psi] & [0] \\ [0] & \alpha_1[\psi]^T[M][\psi] \end{bmatrix} \text{ and } [R] = \gamma[\hat{R}] \tag{3.54}$$

where *M*, *K*, and $\psi$ are the global mass, stiffness and mode shape matrices respectively. $[\hat{R}]$ is considered as identity matrix and $\alpha_1, \alpha_2$ and $\gamma$ are the coefficients associated with total kinetic energy, strain energy and input energy respectively and have been determined by trial and error method. The modified input can be written as

$$\mathrm{v}(t) = u(t) - G_c X \tag{3.55}$$

The closed loop responses can be determined as follows

$$\dot{X} = (A - BG_c)X + Bu \tag{3.56}$$

The energy coefficients ( $\alpha_1, \alpha_2$ and $\gamma$ ) are selected by random numbers within the specified ranges which are determined by trial and error method.

## 3.9 Summary

This chapter deals with the mathematical formulation of dynamic equation of motion of the flexible composite single and double link manipulators based on the Hamilton principle. A three noded layered composite beam element has been implemented based on the Timoshenko beam theory to model and analyse of such manipulator system. The equation of motion has been converted to state space model to obtain the dynamic responses of the flexible manipulators and the formulations of the end effectors based on input shaper and LQR control scheme have also been presented

# Chapter 4

## 4 Results and Discussions

Based on above mentioned formulations in chapter 3 of flexible composite manipulator a complete MATLAB code has been developed and validated with the available results obtained by analytical method and literatures. After validating free and forced vibration analysis has been carried out and presented in the following subsections. The material properties for the convergence study, validation, static and dynamic analysis of the present study are given in Table 4.1.

**Table 4.1. Properties of graphite/epoxy (T300/5208) and kevlar/epoxy (Kevlar 49) [43]**

| Material | Longitudinal Young's modulus $E_{xx}$ (GPa) | Transverse Young's modulus $E_{yy}$(GPa) | Shear modulus $G_{xy}$(GPa) | Shear modulus $G_{yy}$(GPa) | Poisson's ratio$\vartheta$ | Density $\rho$(kg/m$^3$) |
|---|---|---|---|---|---|---|
| Graphite epoxy | 181 | 10.3 | 7.17 | 7.17 | .28 | 1600 |
| Kevlar epoxy | 76 | 5.5 | 2.3 | 2.3 | .34 | 1360 |

### 4.1 Convergence Study

For the convergence study of the present finite element formulation, the graphite/epoxy composite with 16 layers having stacking sequence of [0/ -45/ 45/ 90/ 0/-45/45/90]s has been considered. The first flexural natural frequency of the composite beam with different number of elements is shown in Fig.4.1.

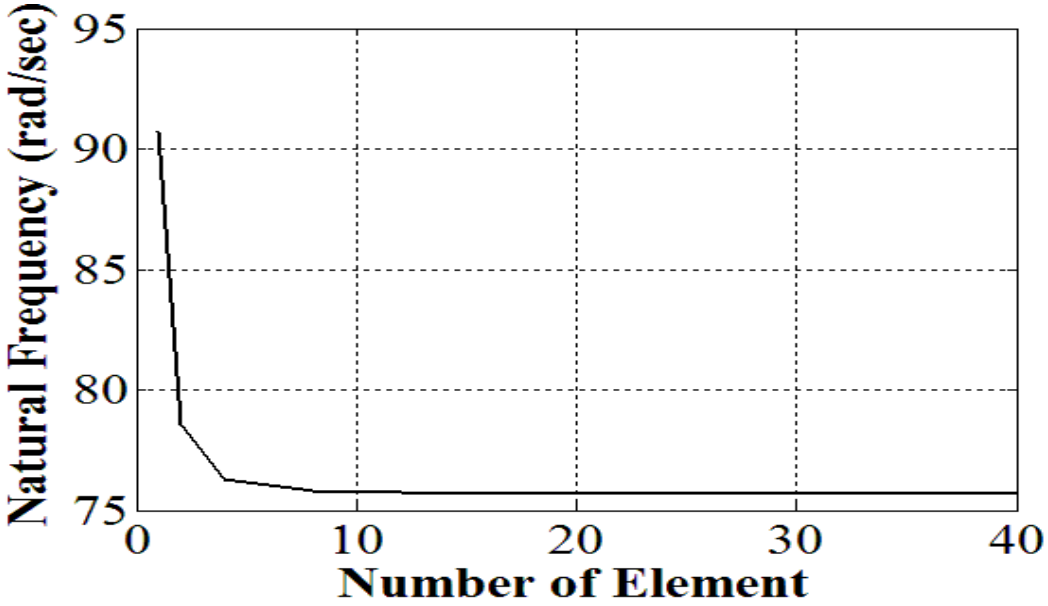


**Fig. 4.1 Natural frequency Vs. Number of element**

It has been cleared from Fig.4.1 that the frequency started converging after taking 16 elements to 0.7570 kHz. For better accuracy for whole present analysis has been carried out considering 20 elements.

## 4.2 Validation

In order to validate the present finite element code, a cantilever beam has been considered. The natural frequency of cantilever beam of isotropic material using classical method can be obtained as follows

$$\omega_n = \beta_i^2 \sqrt{\frac{EI}{\rho A}} \qquad \beta_i L = 1.876;\ \ 4.733;\ \ 7.855 \tag{4.1}$$

**Table 4.2. Validation of result**

| Fundamental frequencies | Classical theory | Present finite element code | Percentage of error % |
|---|---|---|---|
| First Natural frequency $10^2$(rad/sec) | 1.2690 | 1.2043 | 5 |
| Second Natural frequency $10^2$ (rad/sec) | 8.0775 | 7.5423 | 6.62 |
| Third Natural frequency $10^2$ (rad/sec) | 22.249 | 21.094 | 5.185 |

It is clear from the Table 4.2 that the percentage of deviation for first, second and third natural frequencies obtained from the classical theory and present finite element code are 5, 6.62 and 5.185 respectively.

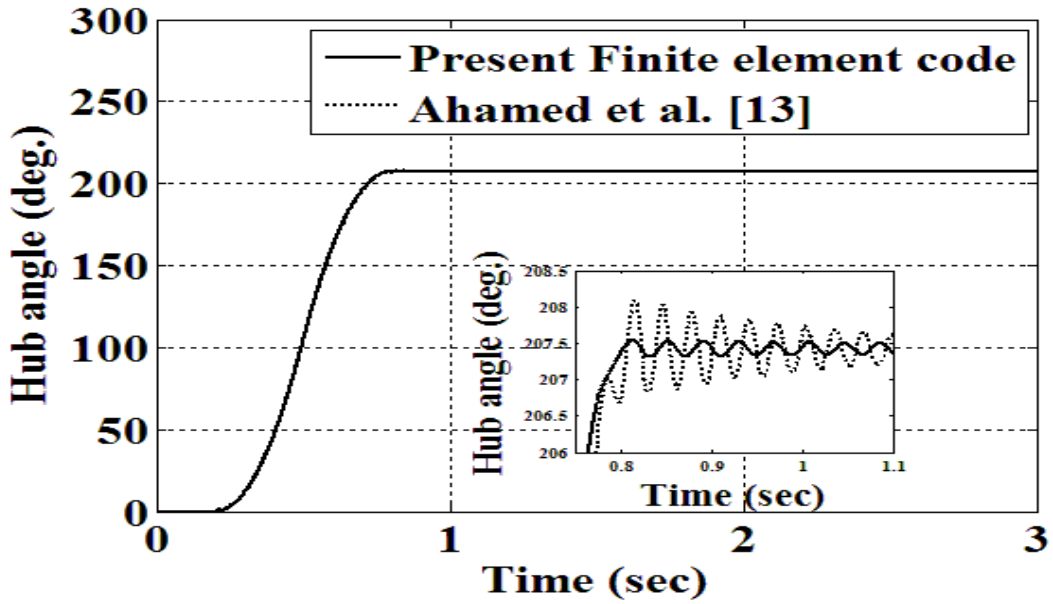


**Fig. 4.2 Validation of result**

It can also be seen from Fig.4.2 that the present formulation is in excellent agreement with the studies by Ahmad et al. [13].

## 4.3 Free Vibration Analysis of Single Link Manipulator with Different Materials

In the present analysis single link manipulator with hollow straight section are considered. The cross section of manipulator consider as a solid circular, with outer diameter 19.008mm. The length of SLFM are 900mm.

**Table 4.3. Comparison of first, second and third natural frequency of single link manipulator considering different materials with different stacking sequences**

| Material | Stacking sequence | First Natural frequency (rad/sec)×$10^3$ | Second Natural frequency (rad/sec) ×$10^3$ | Third Natural frequency (rad/sec) ×$10^3$ |
|---|---|---|---|---|
| **Graphite epoxy (GGGG)** | $[0_G/-45_G/45_G/90_G]_{2s}$ | 0.1055 | 0.7444 | 2.1890 |
| | $[90/45/-45/0/45/0/0/90]_{AS}$ | 0.1104 | 0.7782 | 2.2850 |
| **Graphite/epoxy and Kevlar/epoxy (KGGK1)** | $[0_K/-45_G/45_G/90_G/0_G/-45_G/45_G/90_G]_s$ | 0.1005 | 0.7277 | 2.1558 |
| | $[90/45/-45/0/45/0/0/90]_{AS}$ | 0.1116 | 0.8071 | 2.3856 |
| **Graphite/epoxy and Kevlar/epoxy (KGGK2)** | $[0_K/-45_K/45_K/90_K/0_G/-45_G/45_G/90_G]_s$ | 0.0854 | 0.6189 | 1.8341 |
| | $[90/45/-45/0/45/0/0/90]_{AS}$ | 0.0909 | 0.6577 | 1.9456 |
| **Graphite/epoxy and Kevlar/epoxy (GKKG2)** | $[0_K/-45_K/45_K/90_K/0_G/-45_G/45_G/90_G]_s$ | 0.0957 | 0.6747 | 1.9820 |
| | $[90/45/-45/0/45/0/0/90]_{AS}$ | 0.0989 | 0.6968 | 2.0440 |
| **Graphite/epoxy and Kevlar/epoxy (GKKG1)** | $[0_K/-45_K/45_K/90_K/0_G/-45_G/45_G/90_G]_s$ | 0.0769 | 0.5424 | 1.5925 |
| | $[90/45/-45/0/45/0/0/90]_{AS}$ | 0.0811 | 0.5720 | 1.6798 |
| **Kevlar/epoxy (KKKK)** | $[0_K/-45_K/45_K/90_K/0_K/-45_K/45_K/90_K]_s$ | 0.0718 | 0.5196 | 1.5381 |
| | $[90/45/-45/0/45/0/0/90]_{AS}$ | 0.0751 | 0.5433 | 1.6053 |
| **Aluminum** | 0 | 0.0890 | 0.5915 | 1.7075 |

From the Table 4.3, it is clear that the natural frequencies influences with the materials as well as changes of stacking sequence. By comparing different type of laminated composite links, it is also observed that the natural frequencies is less for symmetric laminated composites than that of anti-symmetric laminates. The natural frequency is high for the graphite/epoxy composites than that of kevlar/epoxy composites but it is in between for hybrid composites (i.e. combination of graphite/epoxy and kevlar/epoxy).

## 4.4 Response Histories of Flexible Composite Manipulators under Different Input Torques

A flexible composite manipulator which is made up of sixteen layers of kevlar/epoxy materials having stacking sequence of $[0/-45/45/90/0/-45/45/90]_s$ has been analysed under different input torques. The flexible manipulator is driven by different torques at the hub as shown in Fig.4.3 to Fig.4.6. The Fig.4.7 shows the dynamic behaviour of flexible link manipulator system such as end point displacement, hub angle and end point residual histories means (residual vibration of the link is caused by movement of the link, which will create uncertainty of the end point position) under various input torques.

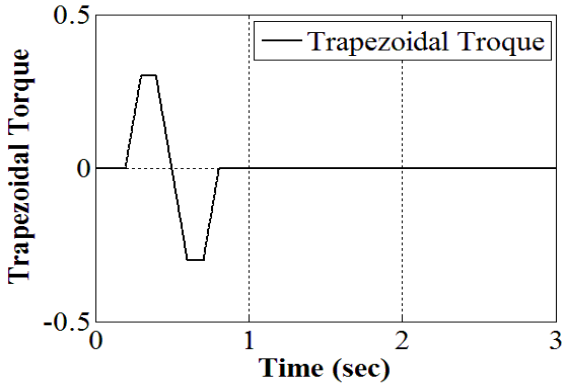


**Fig. 4.3 Trapezoidal torque**

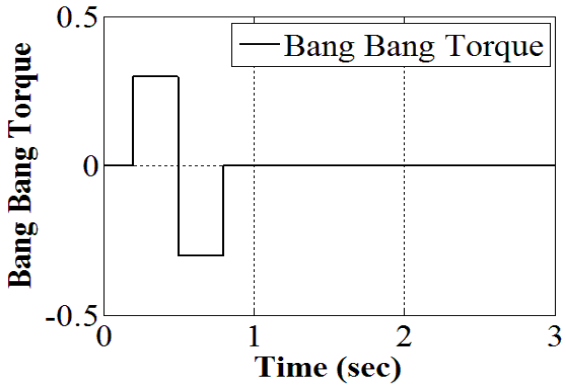


**Fig. 4.4 Bang-Bang torque**

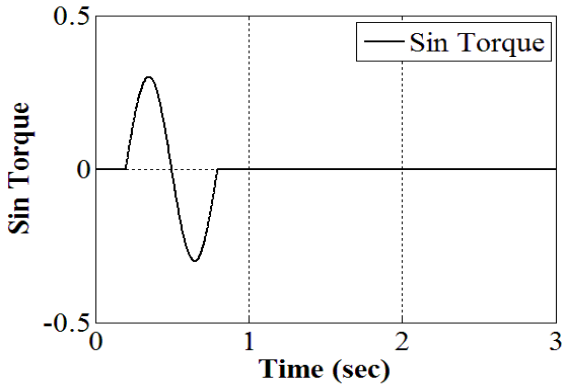


**Fig. 4.5 Sin torque**

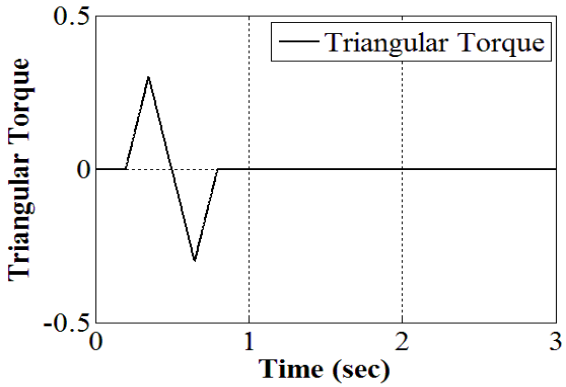


**Fig. 4.6 Triangular torque**

From the Fig.4.7, it is observed that maximum responses for triangular input are less compared to other inputs. It is also clear from the Fig.4.7 that bang-bang torque gives suddenly high end point displacement and hub angle responses, and sin torque may be used for smooth operations of the system but difficultly may arise under the high payload situations whereas trapezoidal torque may prefer because it is better in terms of responses as well as residual vibrations.

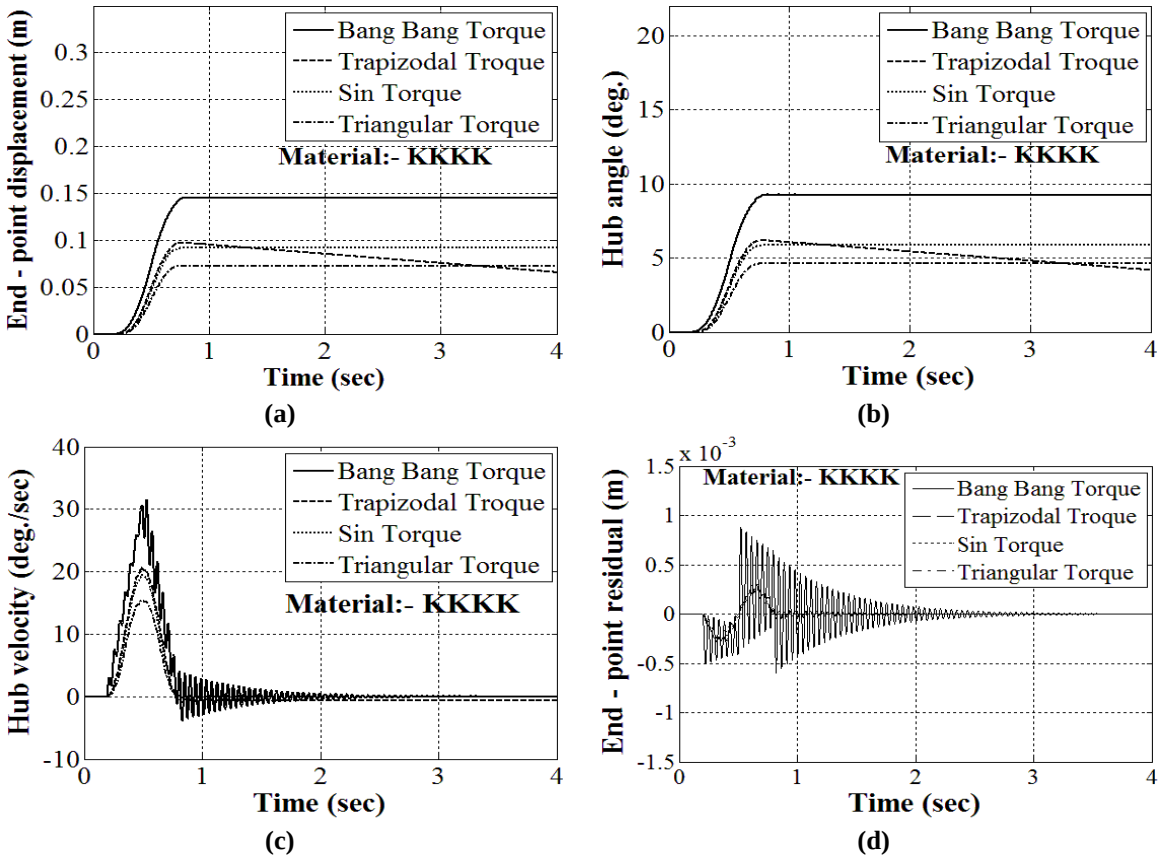


**Fig. 4.7 The comparison of responses of the flexible manipulator under different input torques with payload 90g: (a) End point displacement (b) Hub angle (c) hub velocity (d) end point residual**

## 4.5 Response Histories of the Flexible Manipulator Considering Different Materials

In this analysis, the flexible composite manipulators made by different hybrid composite with stacking sequence of $[0/-45/45/90/\ 0/-45/45/90]_s$ have been analysed under the trapezoidal input torque. In the present analysis flexible manipulator made up of kevlar/epoxy, graphite/epoxy and aluminium are considered. The hybrid laminates is a combination of graphite/epoxy and kevlar/epoxy and four combination of graphite/epoxy and kevlar/epoxy laminates have been considered which are given below.

KGGK1: $[K/G/G/G/G/G/G/G]_s$ KGGK2:$[K/K/K/K/G/G/G/G]_s$

GKKG1: $[G/K/K/K/K/K/K/K]_s$ GKKG2:$[G/G/G/G/K/K/K/K]_s$

Where, K and G stand for kevlar/epoxy and graphite/epoxy ply respectively. The dynamic responses of manipulators under different materials are shown in Fig.4.8 and Fig.4.9. From the Fig.4.8 (a) and (b), it is clear that the displacement as well as hub angle responses increase with more inclusion of kevlar/epoxy layer in the hybrid laminates. It is also observed that end point displacement and hub angle responses are almost equal for GKKG1 hybrid

laminate and considering all layers of kevler/epoxy laminate. It is also apparent from Fig.4.8 (c) that the maximum end point displacement increases with slenderness ratio for all materials. It can also be seen that the maximum end point displacement increases with more inclusion of kevlar/epoxy layer in the hybrid laminates. Hence it can be concluded that flexible manipulator can be more flexible by inclusion of kevlar/epoxy in to hybrid laminates.

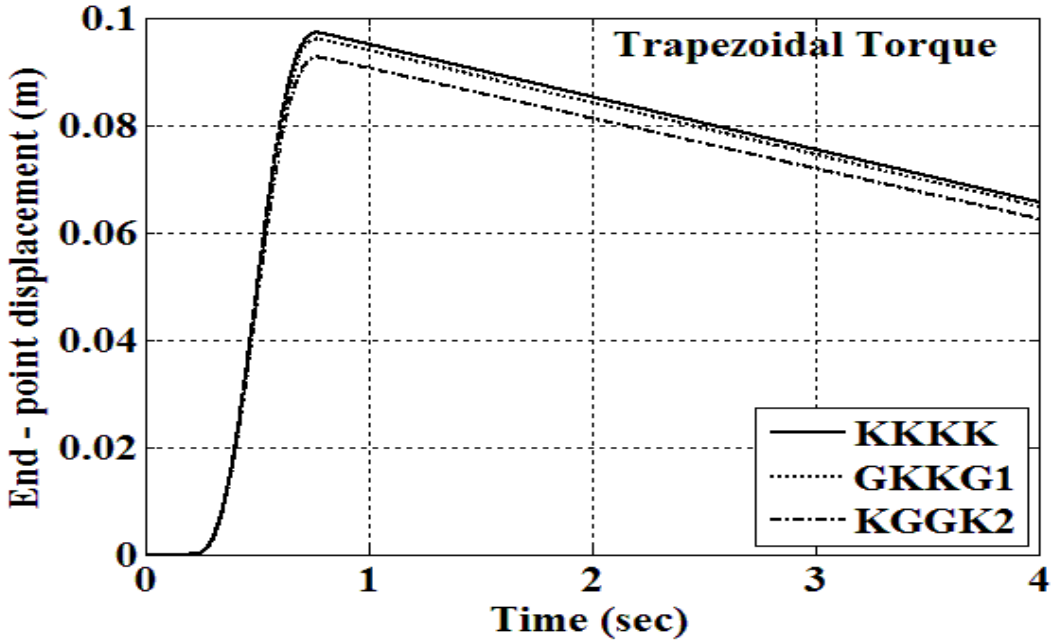


**(a)**

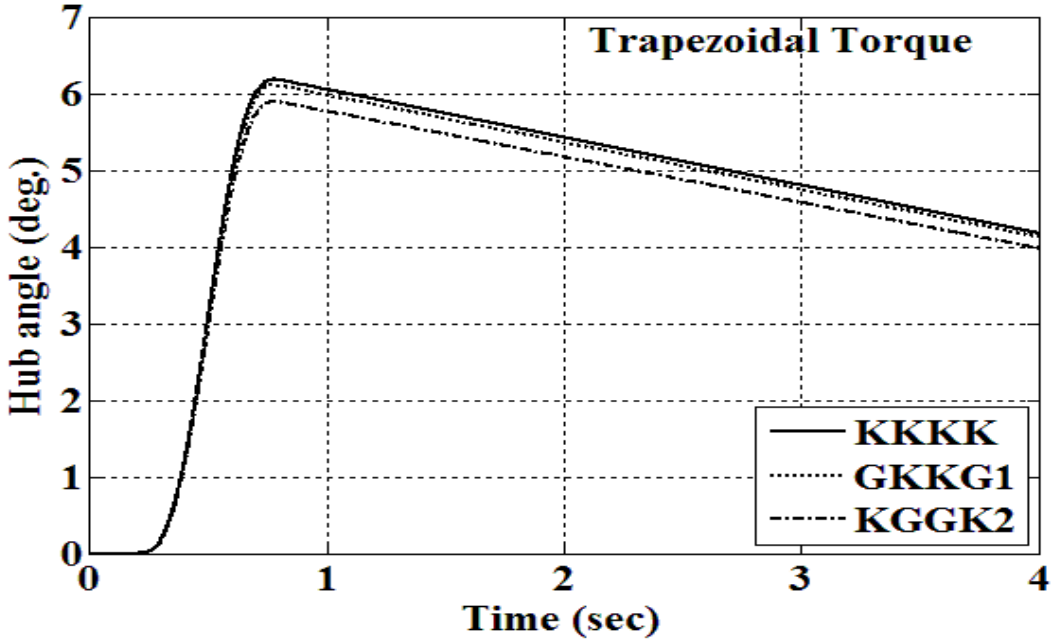


**(b)**

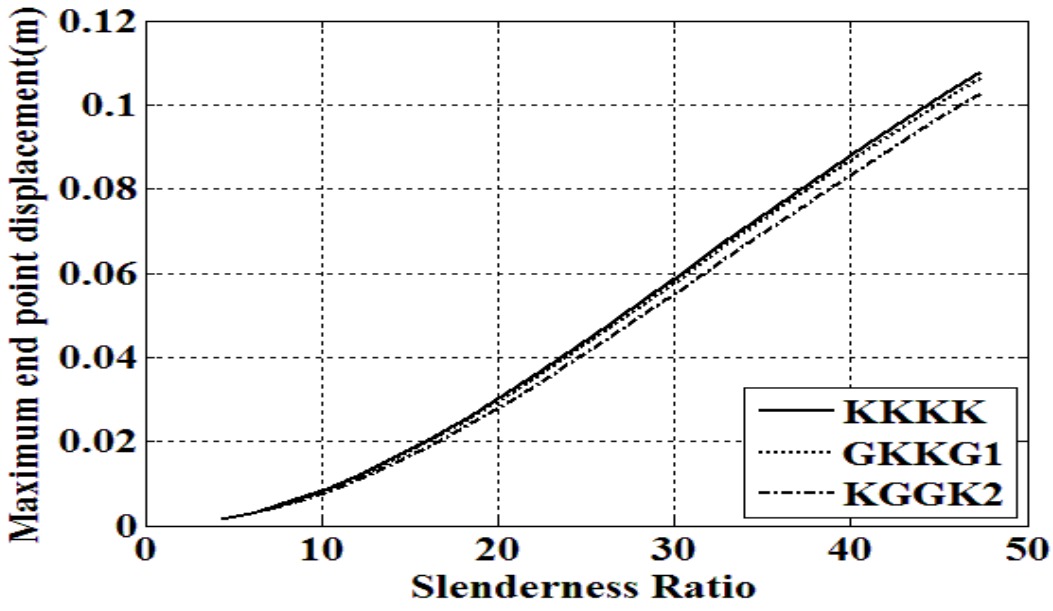


**(c)**

**Fig. 4.8 Responses of kevlar/epoxy hybrid composite manipulators: (a) Displacement histories (b) Hub angle variations (c) the maximum end point displacement vs. various slenderness ratio**

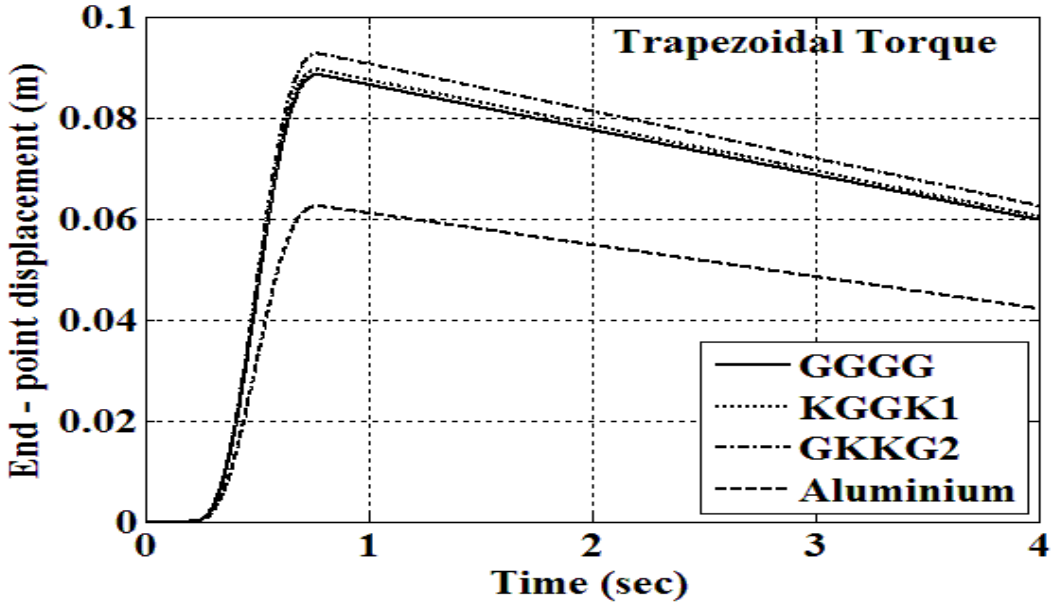


**(a)**

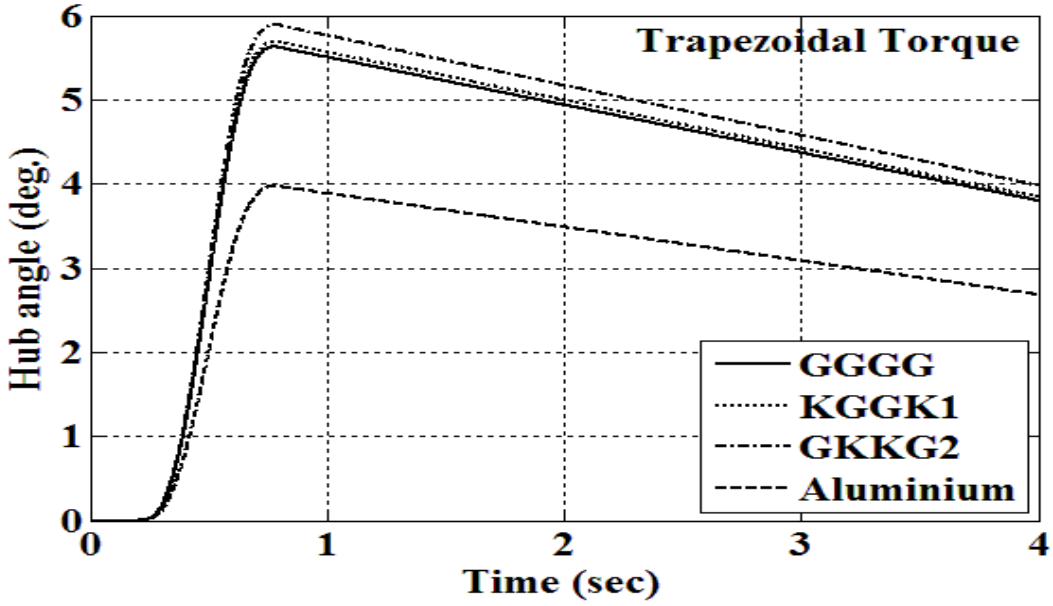


**(b)**

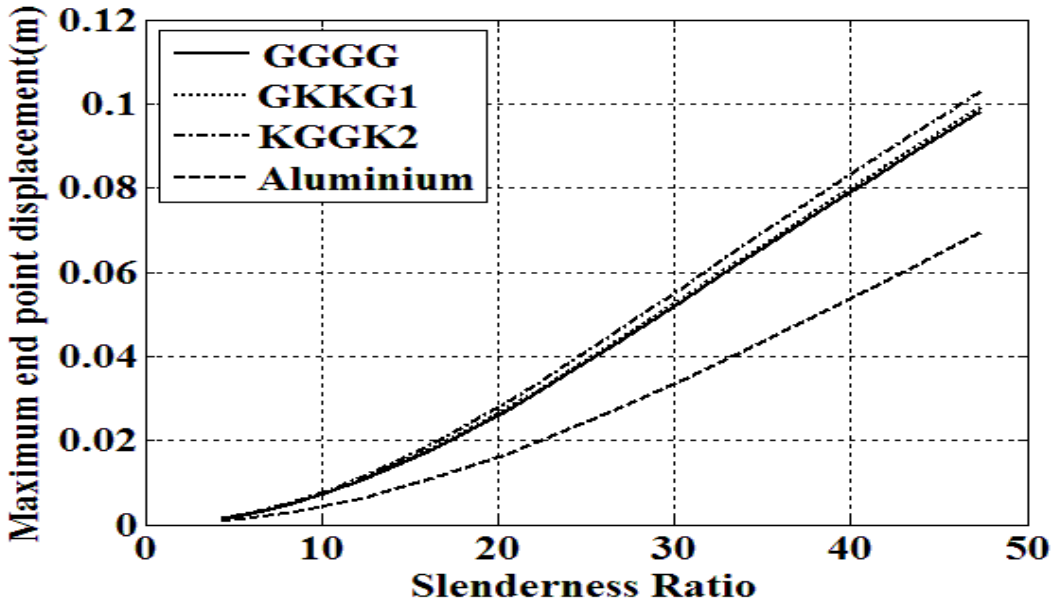


**(c)**

**Fig. 4.9 Responses of graphite/epoxy hybrid composite manipulators: (a) Displacement histories (b) Hub angle variations (c) the maximum end point displacement vs. various slenderness ratio**

For further analysis, Fig.4.9 (a), it is clear that the displacement as well as hub angle decrease with more by inclusion of graphite/epoxy layer in the hybrid laminates. The end point displacement and the hub angle of manipulator is much lower in aluminium as to the composite laminates. It can also be seen that the maximum end point displacement decreases with more inclusion of graphite/epoxy layer in the hybrid laminates. Hence it can be concluded that flexible manipulator is stiffer by inclusion of graphite/epoxy in to the hybrid laminates.

## 4.6 Analysis of Flexible Tapered Single and Double Links Hybrid Composite Manipulators under Trapezoidal Torque

This section concentrates on analysis of hybrid composite manipulators of two types of links, first is solid taper and the second is double tapered single link and double links. For all type of manipulators variation of end point displacement, hub angle response and end point residual with respect to time have also been presented. Finally frequency response of manipulators has also been obtained.

### *4.6.1 Analysis of flexible solid tapered single and double link hybrid composite manipulators under trapezoidal torque*

In the present analysis is used to compare the dynamic responses of the solid tapered single link with solid cross-sections. The GKKG2 hybrid laminate is considered. The taper angles α are varied from 0° to 0.4° (as shown in Fig.4.10). It is clear from the analysis that there is profound effect of the taper angles on dynamic responses of this type of single links (shown in Fig.4.11 (a) and (b)).

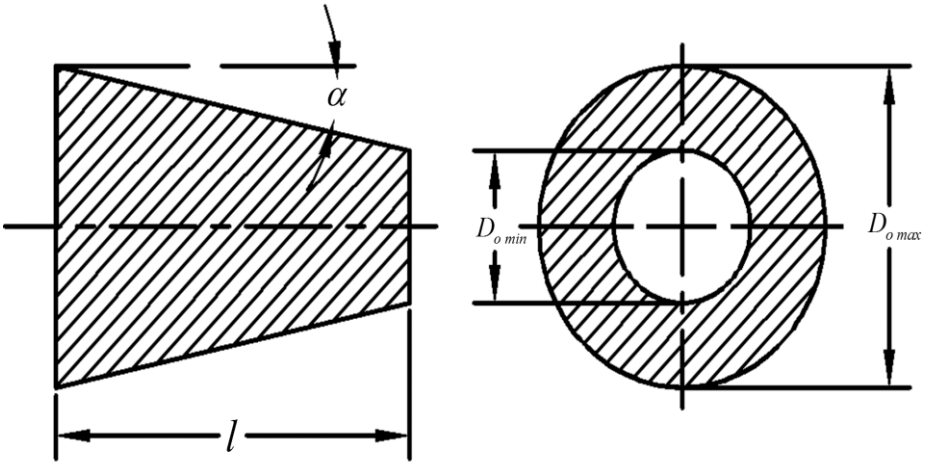


**Fig. 4.10 Variation of solid cross-section along the length of both links by the taper angles α**

It is observed that the maximum end point displacement and hub angle can be obtained for $\alpha$= 0.4° and $\beta$=0°. Figures 4.12 (a) and (b) represent the variation of end point displacement and hub angle respectively with respect to time for particular values of $\alpha$ and $\beta$. Frequency response analysis has also been carried out by applying the magnitude of torque of 0.2 N-m at the hub. Figures 4.12 (c) and (ds) show the end point residual and frequency response residual of the link. It has been observed from the Fig.4.12 (d) that first resonance frequency increases for the taper angles of $\alpha$= *0.4° and* $\beta$=*0°*.

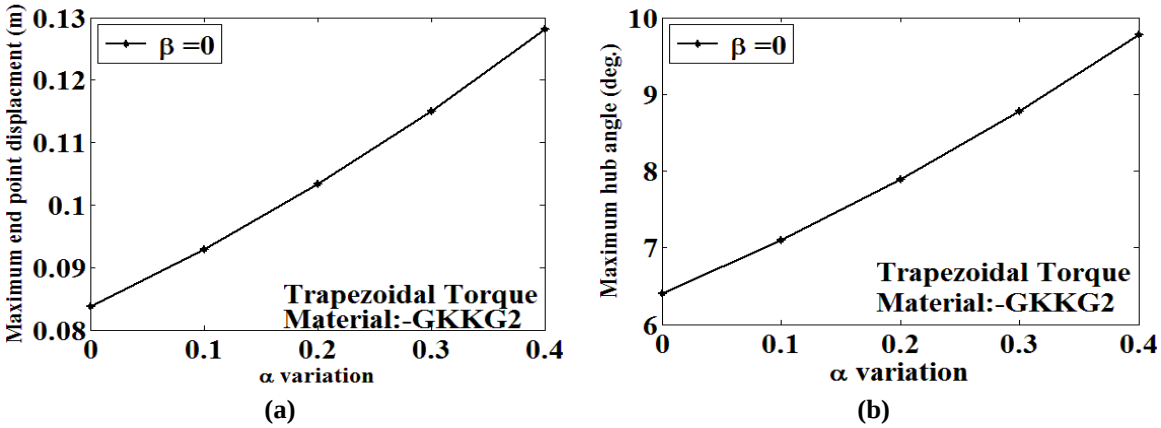


**Fig. 4.11 Variation of maximum endpoint displacement and hub angle response with taper angles**

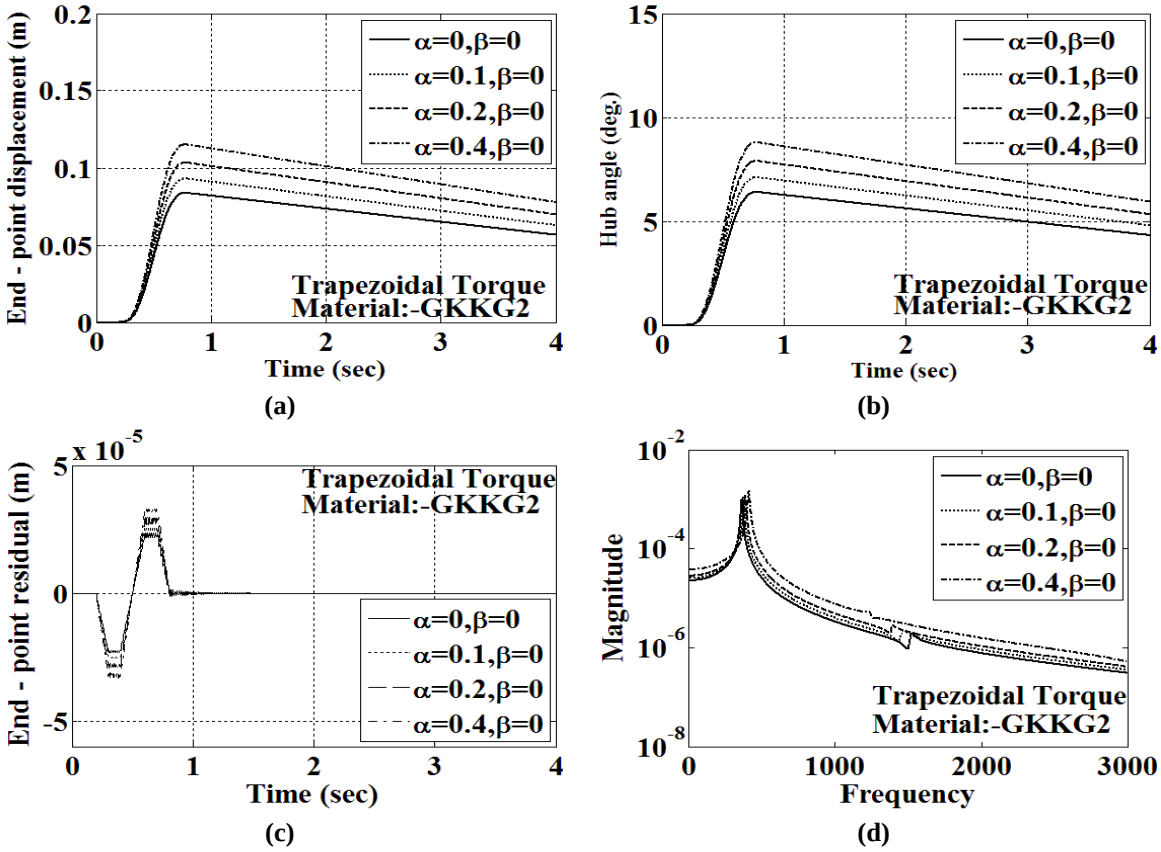


**Fig. 4.12 Comparison of the responses of the single link for particular taper angles: (a) End point displacement (b) Hub angle (c) End point residual and (d) Frequency response of residual**

### *4.6.2 Analysis of flexible solid tapered double link hybrid composite manipulators under trapezoidal torque*

In the present analysis is used to compare the dynamic responses of the tapered double link manipulators with solid cross-sections. The GKKG2 hybrid laminate is considered. The taper angles (both $\alpha$ and $\beta$) are varied from 0° to 0.2°. It is clear from the analysis that there is profound effects of the taper angles on dynamic responses of this type of double links (shown in Fig.4.13 to Fig.4.16).

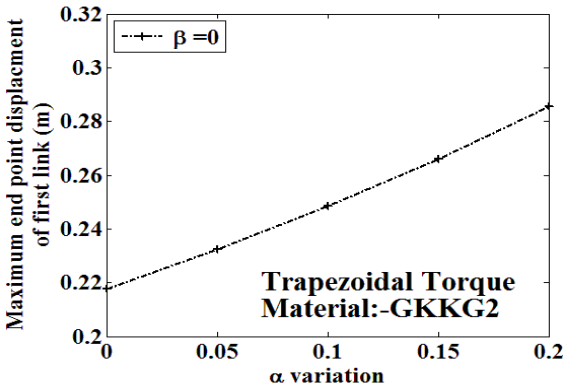


**Fig. 4.13 Variation of maximum endpoint displacement of the first link with taper angles under solid cross section**

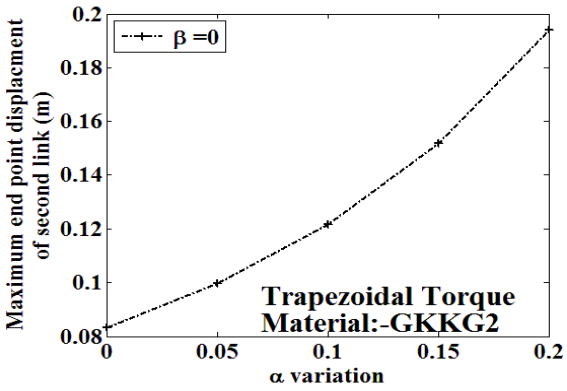


**Fig. 4.14 Variation of maximum endpoint displacement of the second link with taper angles under solid cross section**

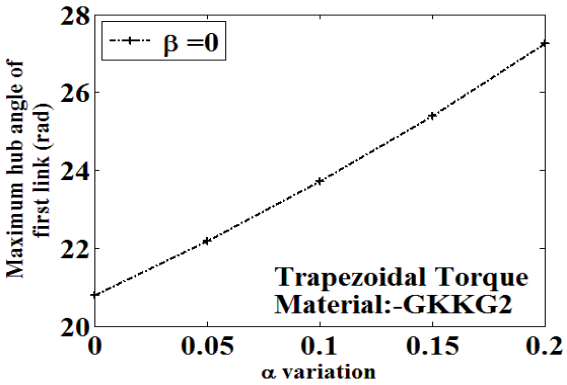


**Fig. 4.15 Variation of maximum hub angle of the first link with taper angles under solid cross section**

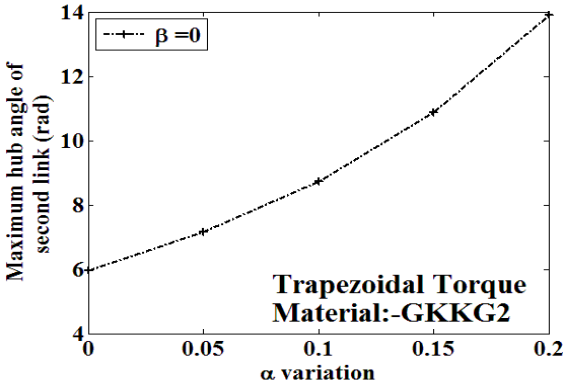


**Fig. 4.16 Variation of maximum hub angle of the second link with taper angles under solid cross section**

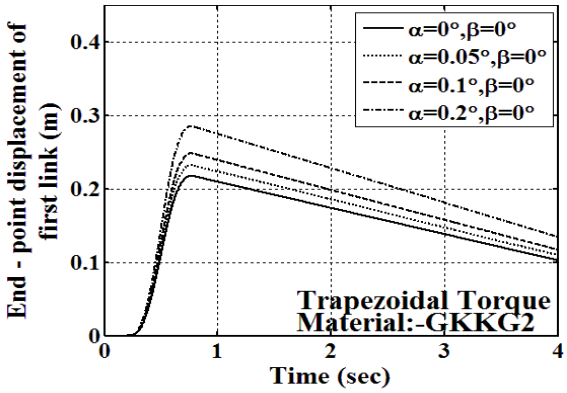


**(a)**

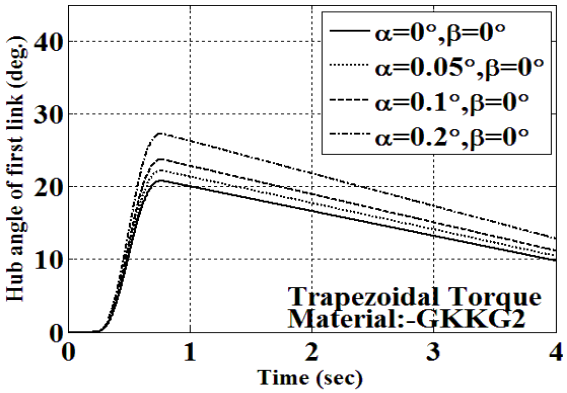


**(b)**

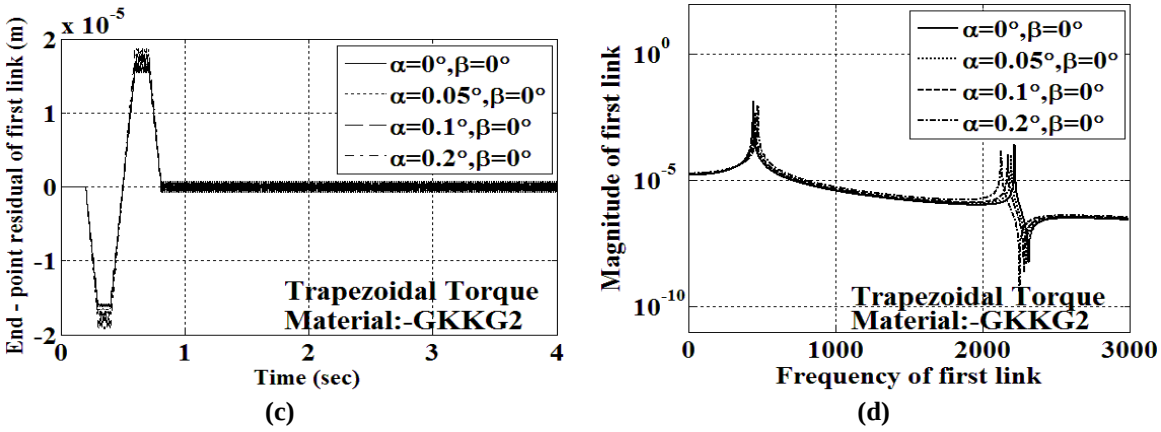


**Fig. 4.17 Comparison of the responses of the first link for particular taper angles in solid cross section: (a) End point displacement (b) Hub angle (c) End point residual and (d) Frequency response of residual**

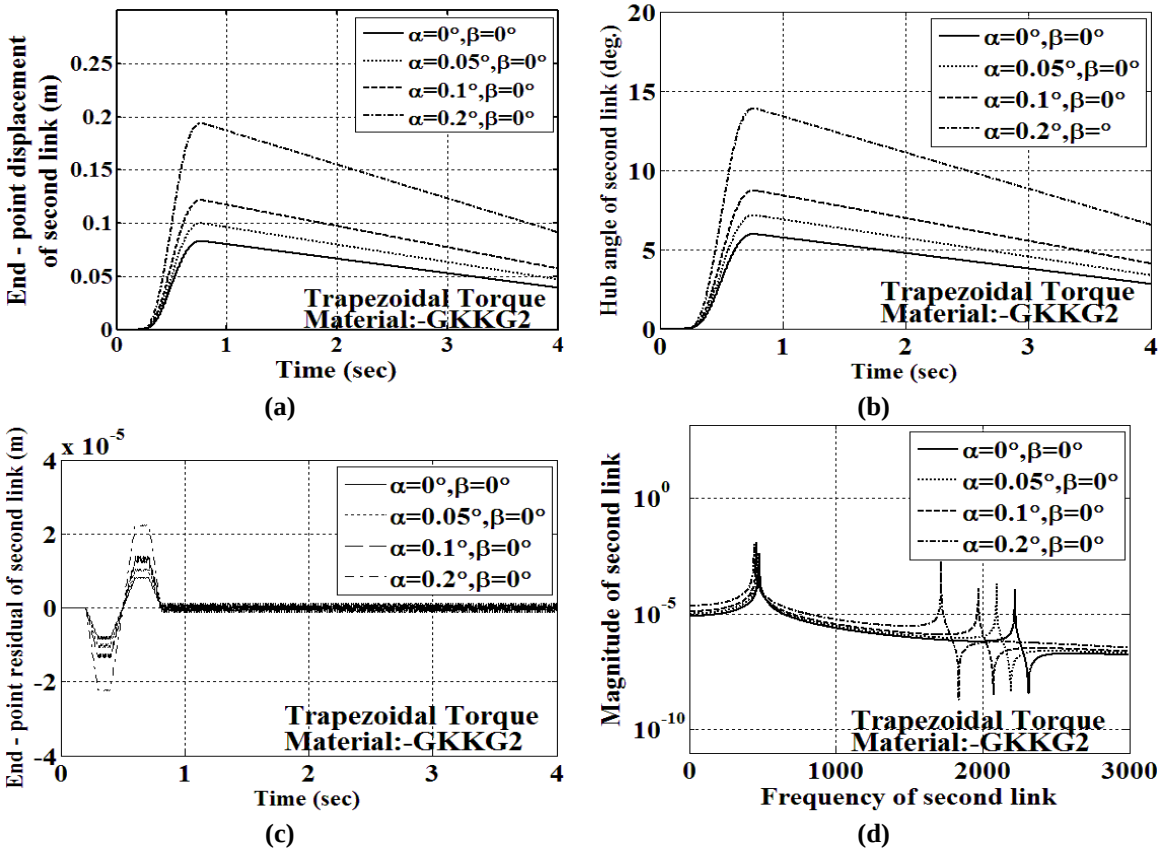


**Fig. 4.18 Comparison of the responses of the second link for particular taper angles in solid cross section: (a) End point displacement (b) Hub angle (c) End point residual and (d) Frequency response of residual**

It is observed that the maximum end point displacement and hub angle can be obtained for $\alpha$=0.2° and $\beta$=0°. Figures 4.17 (a) and (b) represent the variation of end point displacement and hub angle respectively with respect to time for particular values of $\alpha$ and $\beta$. Frequency response analysis has also been carried out by applying the magnitude of torque of 0.2 N-m at the hub. Figures 4.17 (c) and (d) show the end point residual and frequency

response residual of the first link. It has been observed from the Fig.4.17 (d) that first resonance frequency increases for the taper angles of $\alpha$= 0.2° and $\beta$=0°. For $\alpha$= 0.2° and $\beta$=0° section modulus goes on decreasing from the hub to end of the link rapidly than other cases $\alpha$ and $\beta$. Hence the end point residual is maximum for the mentioned value of $\alpha$ and $\beta$. Figures 4.18 (a) and (b) represent the variation of end point displacement and hub angle respectively with respect to time for a particular value of $\alpha$ and $\beta$ for the second link. The rate of variation of end point displacement and hub angle is higher in case of $\alpha$= 0.2° and $\beta$=0°. Figures 4.18 (c) and (d) represent the end point residual and frequency responses of residual of second link. It has also been observed from the Fig. 4.18 (d) that first resonance frequency increases of second link for the taper angles of $\alpha$= 0.2° and $\beta$=0°.

### *4.6.3 Analysis of flexible hollow tapered single link hybrid composite manipulators under trapezoidal torque*

This analysis is used to compare the dynamic responses of the hollow tapered single link with hollow cross-sections. The GKKG2 hybrid laminate is considered. The taper angles (both $\alpha$ and $\beta$) are varied from 0° to 0.4° (as shown in Fig.4.19).

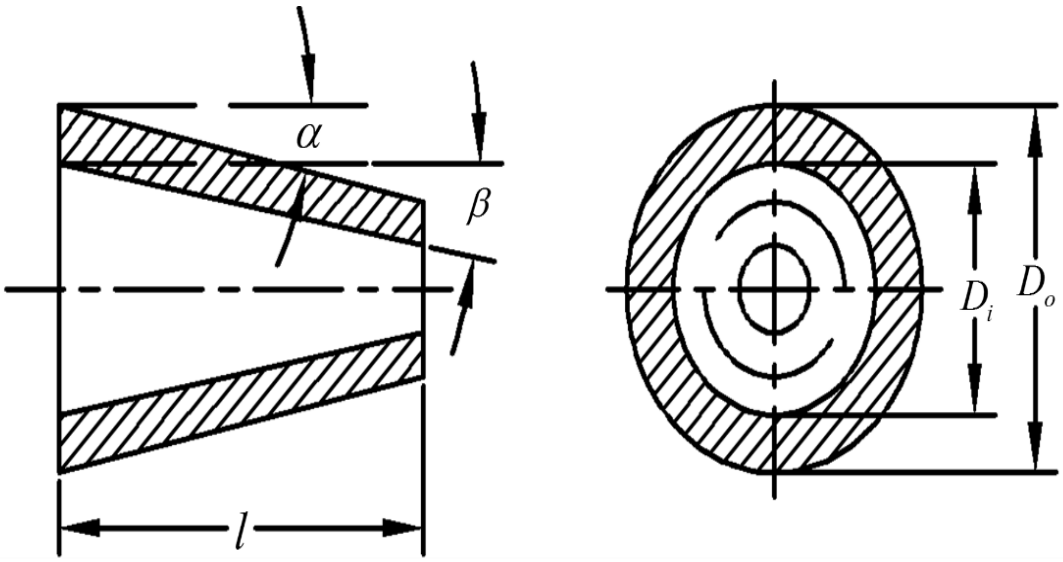


**Fig. 4.19 Variation of hollow cross-section along the length of both links by the taper angles $\alpha$ and $\beta$**

It is clear from the analysis that there is profound effect of the taper angles on dynamic responses of this type of single links (shown in Fig.4.20 (a) and (b)). It is observed that the maximum end point displacement and hub angle can be obtained for $\alpha$= 0.4° and $\beta$= 0°.

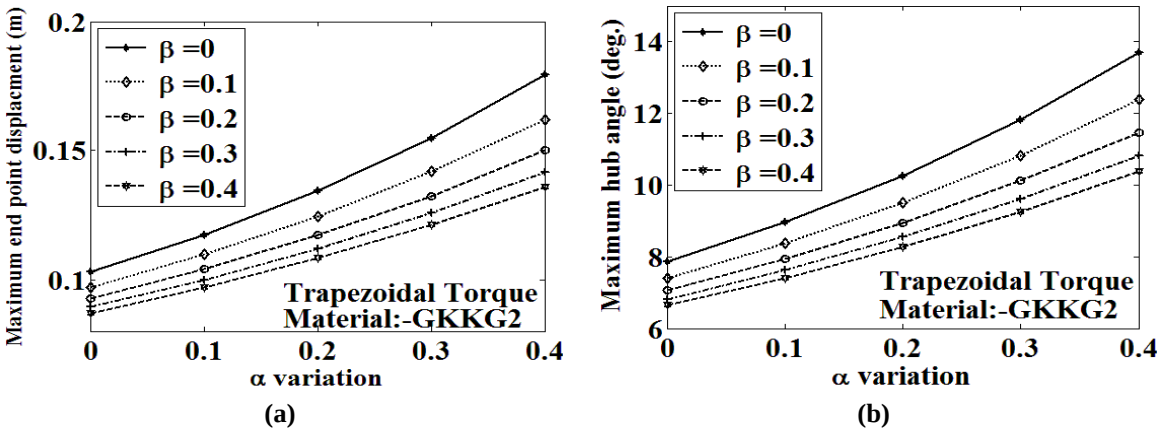


**Fig. 4.20 . Variation of maximum endpoint displacement and hub angle response with taper angles**

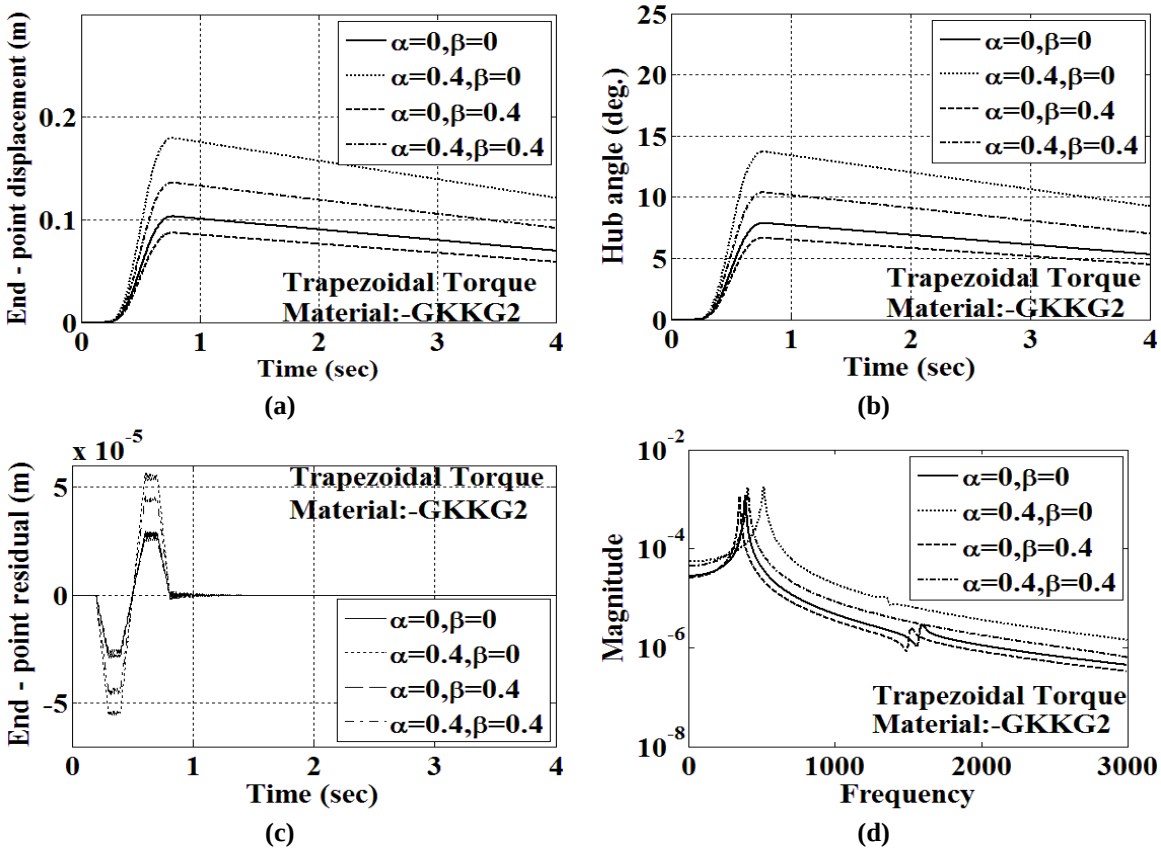


**Fig. 4.21 Comparison of the responses of the single link for particular taper angles: (a) End point displacement (b) Hub angle (c) End point residual and (d) Frequency response of residual**

Figures 4.21 (a) and (b) represent the variation of end point displacement and hub angle respectively with respect to time for particular values of $\alpha$ and $\beta$. Frequency response analysis has also been carried out by applying the magnitude of torque of 0.2 N-m at the hub. Figures 4.21 (c) and (d) show the end point residual and frequency response residual of the link. It has been observed from the Fig.4.21 (d) that first resonance frequency maximum for the taper angles of $\alpha$= 0.4° and $\beta$=0°.

### *4.6.4 Analysis of flexible hollow tapered double link hybrid composite manipulators under trapezoidal torque*

In the present analysis is used to compare the dynamic responses of the tapered double link manipulators with hollow tapered cross-sections. The GKKG2 hybrid laminate is considered. The taper angles (both $\alpha$ and $\beta$) are varied from 0° to 0.2°. It is clear from the analysis that there is profound effect of the taper angles on dynamic responses of this type of double links (shown in Fig.4.22 to Fig.4.25).It is observed that the maximum end point displacement and hub angle can be obtained for $\alpha$= 0.2° and $\beta$=0°. Figures 4.26 (a) and (b) represent the variation of end point displacement and hub angle respectively with respect to time for particular values of $\alpha$ and $\beta$. Frequency response analysis has also been carried out by applying the magnitude of torque of 0.2 N-m at the hub. Figures 4.26 (c) and (d) show the end point residual and frequency response residual of the first link. It has been observed from the Fig.4.26 (d) that first resonance frequency increases for the taper angles of $\alpha$= 0.2° and $\beta$=0°.

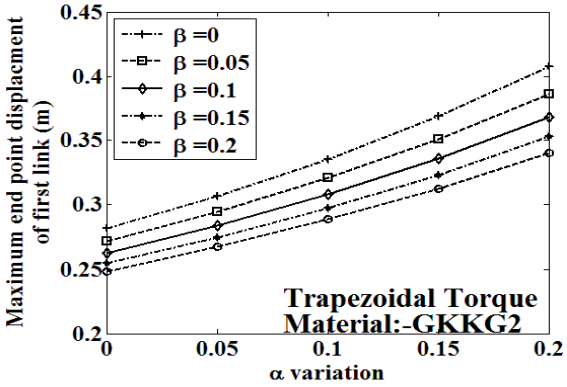


**Fig. 4.22 Variation of maximum endpoint displacement of the first link with taper angles**

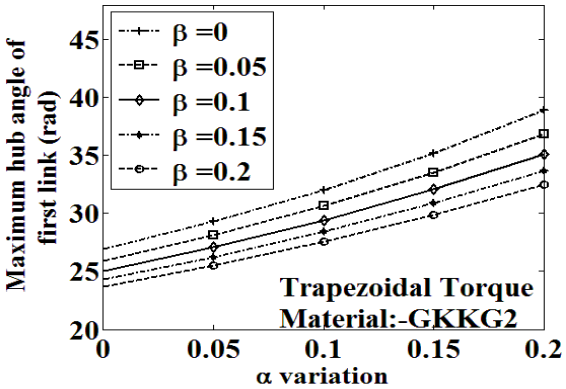


**Fig. 4.23 Variation of maximum hub angle of the first link with taper angles**

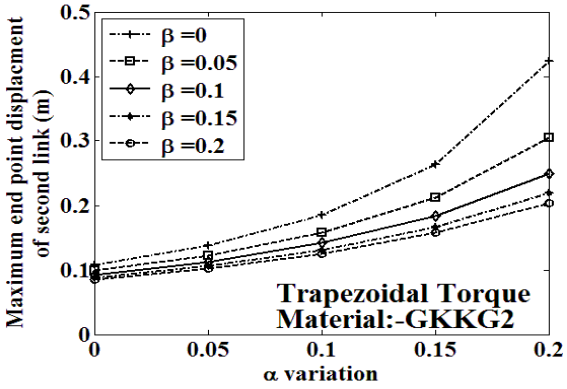


**Fig. 4.24 Variation of maximum endpoint displacement of the second link with taper angles**

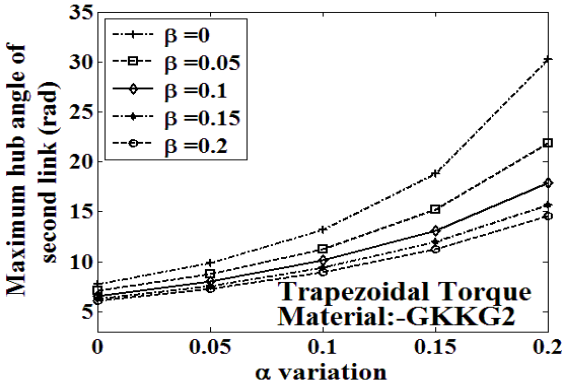


**Fig. 4.25 Variation of maximum hub angle of the second link with taper angles**

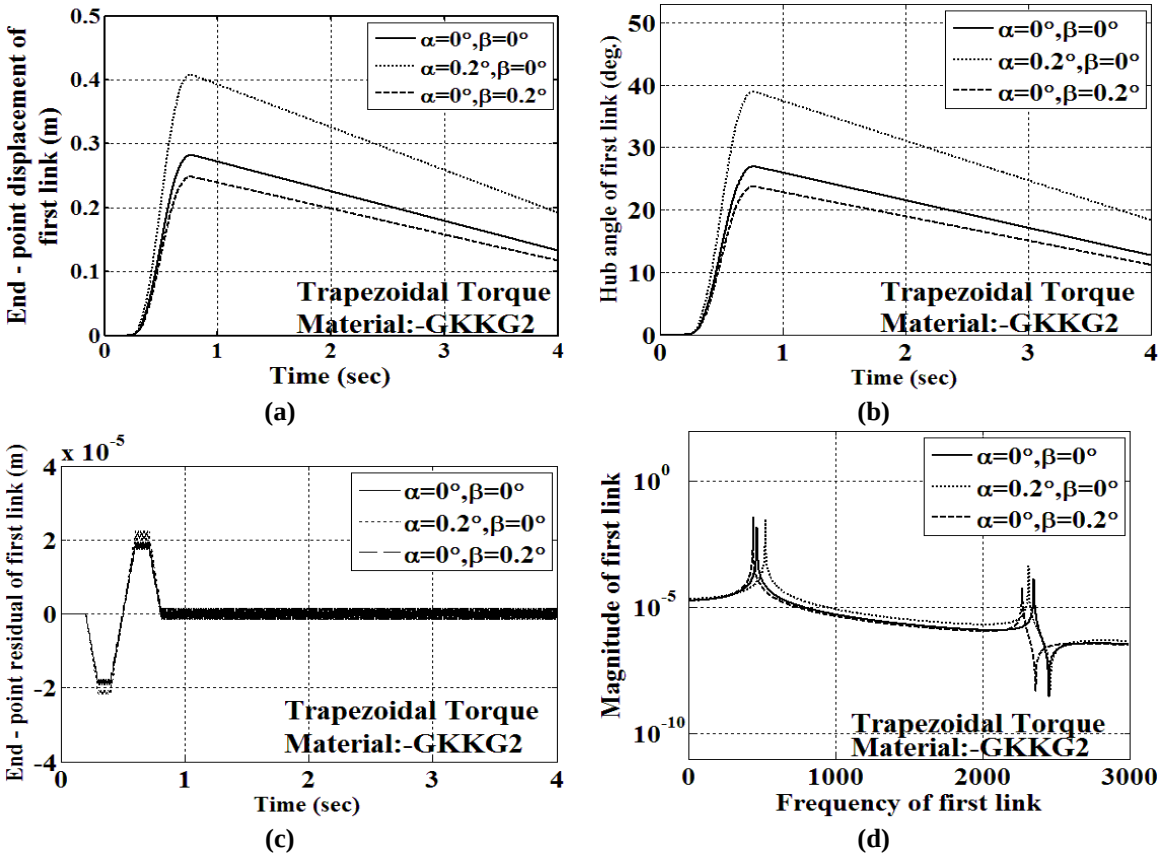


**Fig. 4.26 Comparison of the responses of the first link for particular taper angles: (a) End point displacement (b) Hub angle (c) End point residual and (d) Frequency response of residual**

For $\alpha$= 0.2° and $\beta$=0° section modulus goes on decreasing from the hub to end of the link rapidly than other cases $\alpha$ and $\beta$. Hence the end point residual is maximum for the mentioned value of $\alpha$ and $\beta$. Figures 4.27 (a) and (b) represent the variation of end point displacement and hub angle respectively with respect to time for a particular value of $\alpha$ and $\beta$ for the second link. The rate of variation of end point displacement and hub angle is higher in case of $\alpha$= 0.2° and $\beta$=0°.

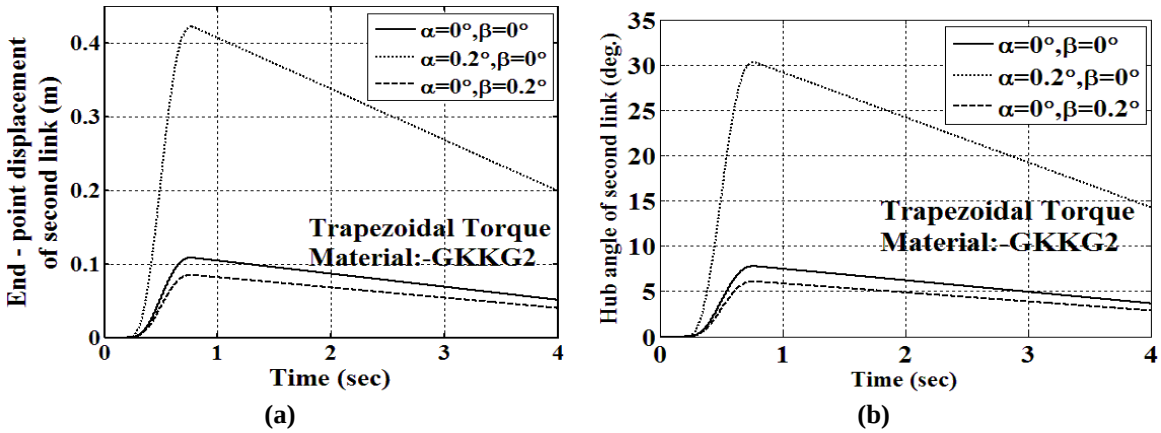

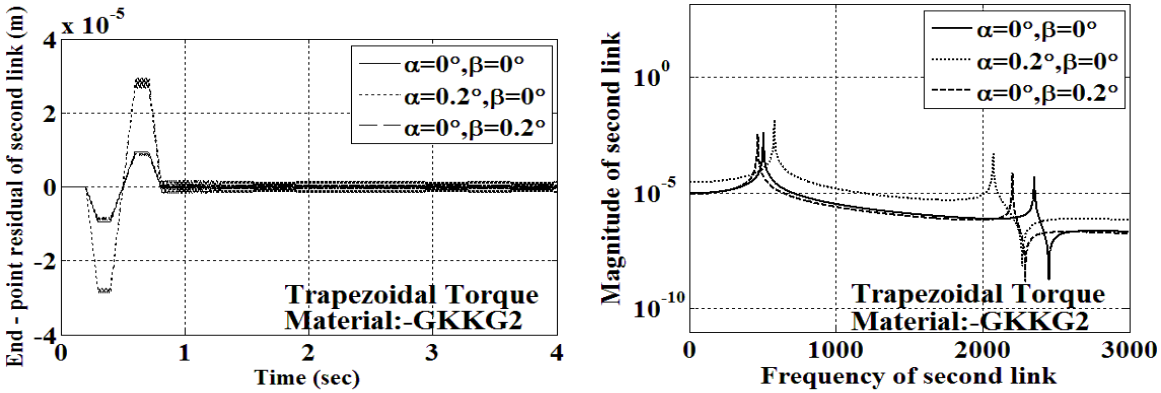


**Fig. 4.27 Comparison of the responses of the second link for particular taper angles: (a) End point displacement (b) Hub angle (c) End point residual and (d) Frequency response of residual**

Figures 4.27 (c) and (d) represent the end point residual and frequency responses of residual of second link. It has also been observed from the Fig.4.27 (d) that first resonance frequency increases of second link for the taper angles of $\alpha$= 0.2° and $\beta$=0°.

## 4.7 Responses of Flexible Tapered Single and Double Links Hybrid Composite Manipulator based on the Input Shaping of Trapezoidal Torque

In this study mainly focus on the design of the input shaper on the single and double link manipulators. The input shaper designed to reduce the end point residual of the manipulators. The responses of flexible tapered single and double links hybrid composite manipulators have been shown in below. Responses of the manipulators are studied based on variation of the end point displacement, hub angle and end point residual.

### *4.7.1 Responses of flexible tapered single link hybrid composite manipulator based on the input shaping of trapezoidal torque*

The input shaper are designed considering two and three impulse sequences for first three modes of vibrations.

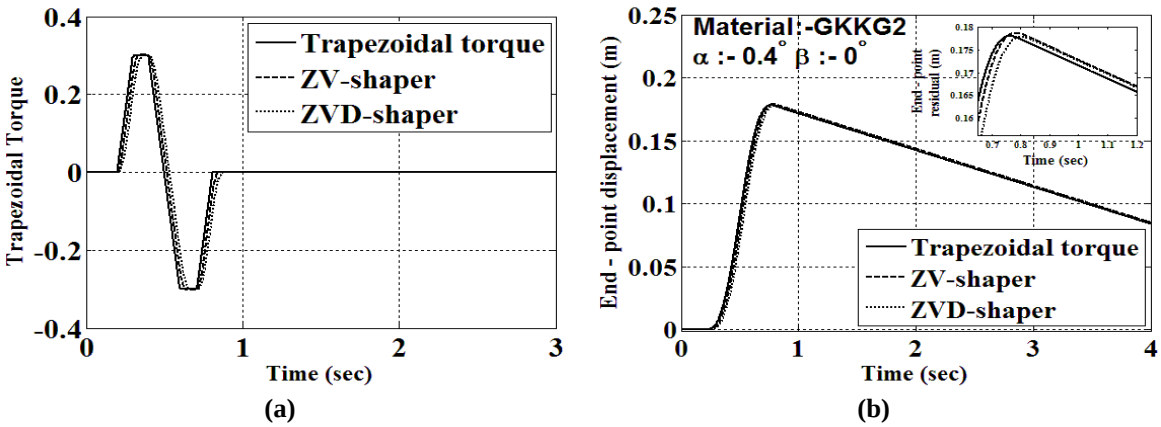

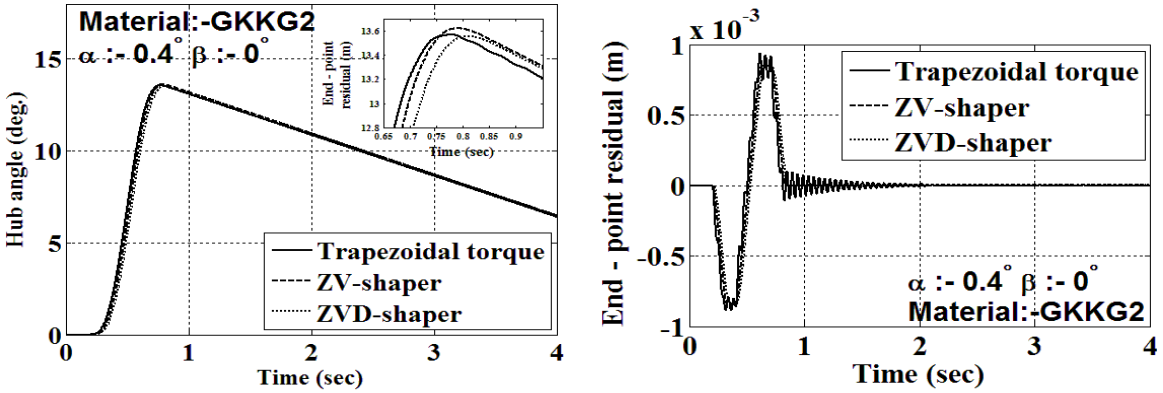


(c) (d)

**Fig. 4.28 Comparison of the responses of flexible tapered hybrid composite manipulator under different input shapers and trapezoidal torque (a) Different torques (b) End point displacement (c) hub angle (d) End point residual.**

The amplitude and time delay are calculated based on the discussion in the subsection 3.7 of chapter 3. The GKKG2 hybrid laminate is considered and the taper angle is taken as $\alpha$=0.4° and $\beta$=0°. The trapezoidal torque, different input shapers and dynamic responses of this flexible manipulator are shown in Fig.4.28. From the Fig.4.28, It has been observed that the maximum end point displacement and hub angle responses is almost same considering ZV and ZVD shapers but the end point residual vibration is less while considering the input shapers. The end point residual vibration is less in case of ZVD input shaper compared to ZV input shaper.

### *4.7.2 Responses of flexible tapered double links hybrid composite manipulator based on the input shaping of trapezoidal torque*

In the present study, a flexible tapered double links hybrid composite manipulator is also analysed under different input shapers. The same taper angle and hybrid laminate are considered as single link. The responses of this flexible link under different input shapers compared to trapezoidal torque is depicted in the Fig.4.29. From the Fig.4.29, it can be observed that the smoothening effects is more in case of second link than that of first link.

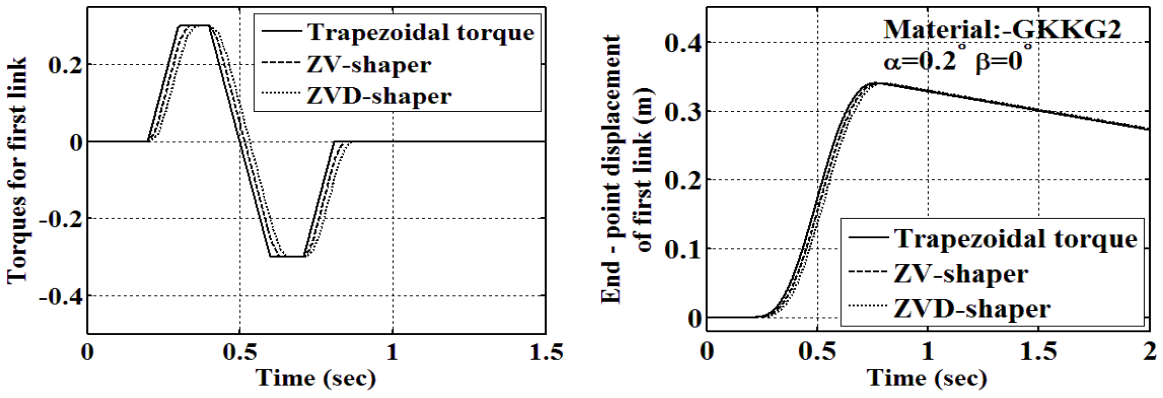


(a) (b)

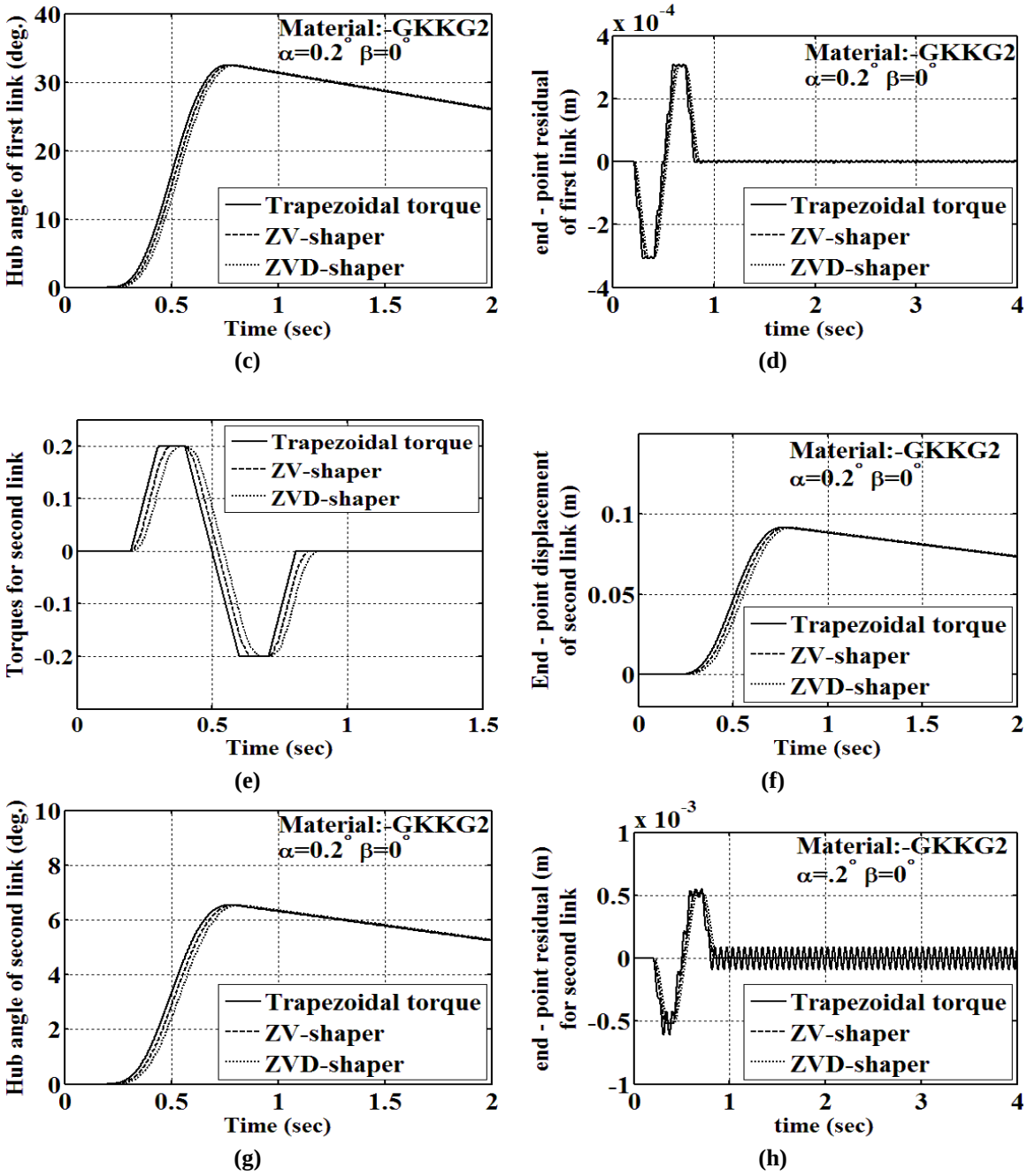


**Fig. 4.29 Comparison of the responses of flexible tapered hybrid composite manipulator under different input shapers and trapezoidal torque (a) Different Torques for first link (b) End point displacement for first link (c) hub angle for first link (d) End point residual for first link (e) Different Torques for second link (f) End point displacement for second link (g) hub angle for second link (h) End point residual for second link**

It is also found that the smoothening effect is more while using ZVD shaper compared to ZV shaper. The residual is more for first link than second link this may due to inertial effect of first link.

## 4.8 Controlled Responses of Flexible Tapered Double Links Hybrid Composite Manipulator using LQR Scheme

In the present study, a flexible tapered double links hybrid composite manipulator is considered to study the control performances and responses using present LQR control scheme. The manipulator has been driven by ZVD shaper.

### *4.8.1 Responses of flexible hollow tapered double links hybrid composite manipulator using LQR scheme*

The Fig.4.30 (a) and (b) show that control input and responses of the first link for different values of energy coefficients. The Fig.4.30 (c) and (d) show that control input and responses of the second link for different values of energy coefficients.

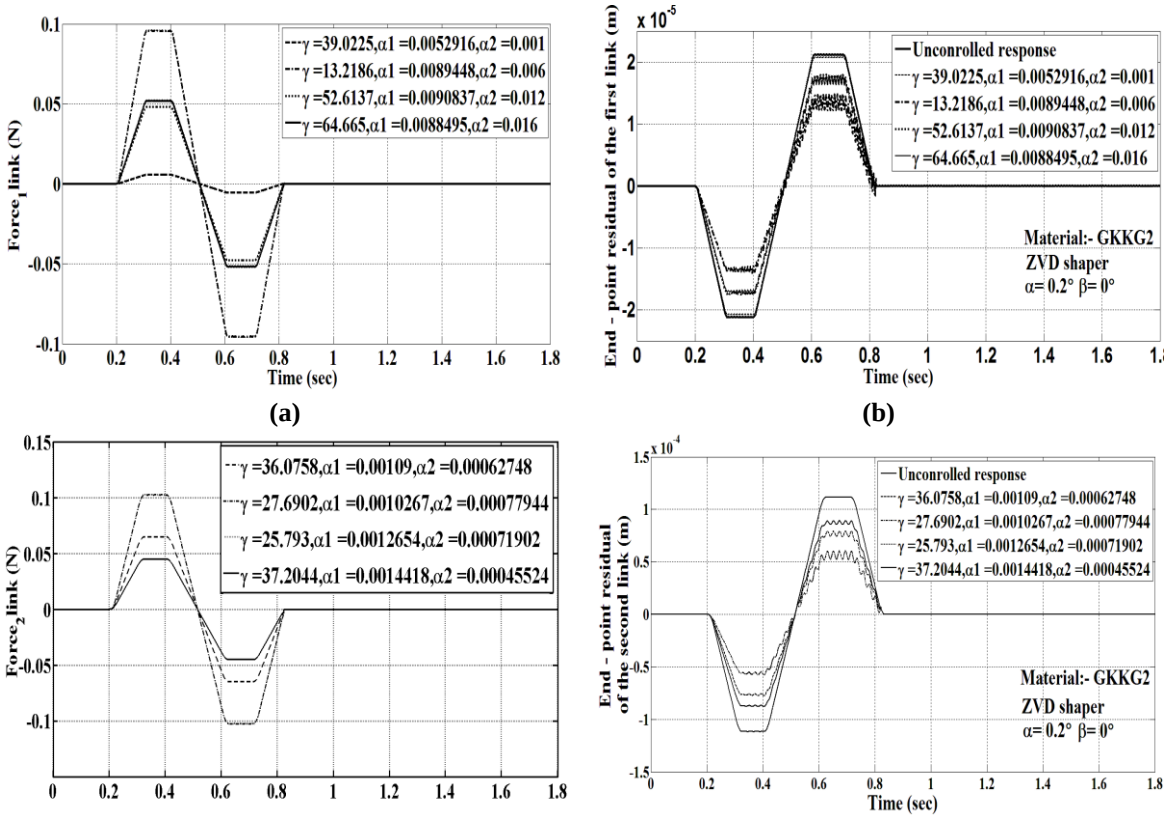


**Fig. 4.30 Comparison of the end point residual and control input of the flexible hollow tapered hybrid composite manipulator using LQR controller with energy coefficients $\alpha_1, \alpha_2$ and $\gamma$ : (a) Control input for first link (b) Uncontrolled and controlled residuals of first link (c) Control input for second link (d) Uncontrolled and controlled residuals of second link**

It has been observed from the Fig.4.30 that the present LQR control scheme is capable to control the end effector residuals with less control efforts.

### *4.8.2 Responses of flexible solid tapered double links hybrid composite manipulator using LQR scheme*

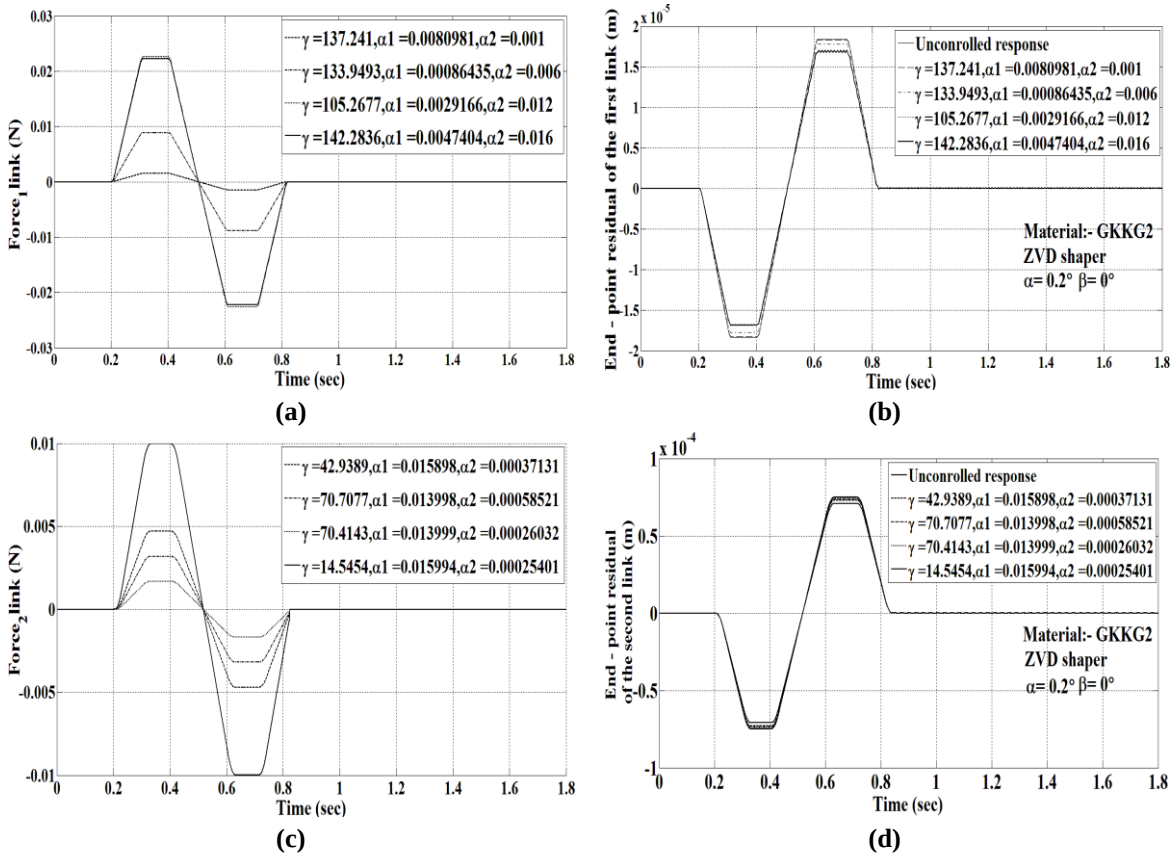


**Fig. 4.31 Comparison of the end point residual and control input of the flexible solid tapered hybrid composite manipulator using LQR controller with energy coefficients $\alpha_1, \alpha_2$ and $\gamma$ : (a) Control input for first link (b) Uncontrolled and controlled residuals of first link (c) Control input for second link (d) Uncontrolled and controlled residuals of second link.**

The Fig.4.31 (a) and (b) show that control input and responses of the first link for different values of energy coefficients. The Fig.4.31 (c) and (d) show that control input and responses of the second link for different values of energy coefficients. It has been observed from the Fig.4.31 that the present LQR control scheme is capable to control the end effector residuals with less control efforts

## 4.9 Summary

In this present chapter first the convergence study has been carried out and it has been found that the results from presented code are converged at 16 elements. Then the results have been validated with analytical method and also from available results in the literature. It has been observed that obtained result from present computer code based on the present formulations are an excellent agreement with the analytical as well as already published results [13].

The free vibration analysis have been carried out considering symmetric and anti-symmetric hybrid composite laminates. It has been found that the natural frequency of the system is less under the symmetric laminates and also the natural frequency is high for graphite/epoxy laminates. The inclusion of the kevlar/epoxy layer into hybrid composite the natural frequency of the system decreases.

The dynamic analysis of the flexible manipulator considering different parameters are also studied. Firstly the dynamic analysis of the single link manipulator under different torque are carried out. It has been found that the trapezoidal torque has better performance than that of other torques. The dynamic analysis of the single link manipulator for different materials has also been carried out. By the inclusion of the kevlar/epoxy into the hybrid composite the results in increase of response of the single link manipulator. It has also been found that it is better to make inner layers softer by kevlar/epoxy layers and outer surfaces stronger by graphite/epoxy layers. The dynamic analysis also reveal that the end point displacement for link with $\alpha$=.4° and $\beta$=0° is more than that of link with other configuration including solid links. It has also been observed that the responses of the flexible manipulator is high under the condition of tapered hollow cross-sections. The responses of the manipulator under the input shaper have also been analysed. It has been observed that the developed input shaping scheme is efficient to reduce the end point vibration of the flexible tapered single and double hybrid composite manipulators without compromising the end effector displacement. The LQR scheme has been applied in order to further reduce the residual vibration of the end effector. It has also been observed that the present LQR control scheme is capable to control the end point residual of the flexible tapered hybrid composite manipulators.

# Chapter 5

# 5 Conclusions and Scope of Future Works

Some important observations based on the formulation and results obtained are presented here and the scope of future works also encapsulated at the end of this chapter.

## 5.1 Conclusions

A three noded beam element has been implemented based on the Timoshenko beam theory for modelling and analysis of the flexible composite manipulators under different input torques. The developed layered beam element can model the flexible manipulators for any number of layers and composite materials. The single and double link manipulators are modelled based on the finite element method. Such systems are then simulated under the different input torques using MATLAB and the responses are analysed. Various analysis of the flexible single and double links have been carried out. Important conclusions obtained from the present study have been presented as follows:

i. Convergence study of present FE model has been done for the first natural frequency of the manipulator with number of elements. It has been found that first natural frequency is coverged after 16 elements.

ii. It has been found from free vibration analysis that there is profound effect on the natural frequencies of flexible composite manipulator with different stacking sequences of the composite layers. It has also been found that the natural frequency has more in the case of graphite/epoxy laminate compare to the kevlar/epoxy laminates. The less natural frequency obtained under the case of symmetric laminates

iii. Responses of the flexible single link composite manipulators due to different input torques have also been analysed and it has been found that the trapezoidal torque has better performance than that of other torques.

iv. Responses of flexible single links composite manipulators considering different type of composite materials ((such as graphite/epoxy and kevlar/epoxy) have also been analysed which reveals that the end point displacement and hub angle variation of the flexible composite manipulator made by graphite/epoxy laminate is less than that of Kevlar/ epoxy laminate.

v. Responses of the single link manipulator with the different hybrid composites laminates (combination of graphite/epoxy and kevlar/epoxy materials) have also been

obtained. It has been found that it is better to make inner layers softer by kevlar/epoxy layers and outer surfaces stronger by graphite/epoxy layers.

vi. Response of flexible manipulator with the aluminum and composite materials has been analyzed, which reveals that the displacement histories and hub angle variation of the flexible composite manipulator made by aluminum is less than that of considered composite laminates.

vii. The effects of taper angles on the responses of tapered solid hybrid composite laminates of the flexible single and double links manipulator have also been analysed. It is observed that for the single link manipulator, the maximum end point displacement and hub angle can be obtained for the taper angles of $\alpha$ = 0.4° and $\beta$=0° and for the double link manipulator can be obtained for the taper angles of $\alpha$ = 0.2° and $\beta$=0°.

viii. The effects of taper angles on the responses of tapered hollow hybrid composite laminates of the flexible single and double links manipulator have also been analysed. It is observed that for the single link manipulator the maximum end point displacement and hub angle can be obtained for the taper angles of $\alpha$ = 0.4° and $\beta$=0° and for the double link manipulator obtained for the taper angles of $\alpha$ = 0.2° and $\beta$=0°. It has also been found that the maximum response of the hollow tapered cross sections is more than the solid tapered cross sections.

ix. The input shaping of the trapezoidal input torque based on the zero vibration (ZV) and zero vibration derivative (ZVD) has also been carried out in order to reduce the residual vibration of the end effector by adjusting the amplitude and time delay. It has been observed that the developed input shaping scheme is efficient to reduce the end point vibration of the flexible tapered hybrid composite manipulators without compromising the end effector displacement and hub angle response.

x. The linear quadratic regulator control (LQR) scheme has been applied in order to further reduce the residual vibration of the end effector. It has also been observed that the present LQR control scheme is capable to control the end point residual of the flexible tapered hybrid composite manipulators.

## 5.2 Scope of Future Works

i. Incorporation of coupled axial, bending and torsion effects considering 3D flexible beam based on the Timoshenko beam theory
ii. Incorporation of non-linearity to the present FE model
iii. Study of delamination of flexible composite manipulator and
iv. Optimal design and control of flexible composite manipulator with sensors and actuators

# List of Publications from Present Research Work

[1] Jefrin Jose P. and Tarapada Roy. Vibration Analysis of Flexible Composite Manipulators, *Advanced Science Letters*(Accepted)

[2] Jefrin Jose P. and Tarapada Roy. Dynamic Analysis of Flexible Composite Manipulator. Sixth International Conference on Theoretical, Applied, Computational and Experimental Mechanics, (December 29, 2014- December 31, 2014), IIT Kargpur

[3] Jefrin Jose P. and Tarapada Roy. Dynamic and Control of Flexible Double Tapered Two Links Hybrid Composite Manipulators, Journal of Structural Stabity and Dynamics (Submitted), 2015

# Referensce


[1] Ata A A, Haraz H E, Rizk E A A and Hanna N S. Kinematic Analysis of Single Link Flexible Manipulator. International Conference on Information Technology, *IEEE* 2012.

[2] Kumar K K, Srinath A, Anvesh J G, Pram R and Suresh M. Kineamtic Analysis and Simulation of 6 Dof KukaKr5 Robot for Welding Application. International Journal of Engineering Research and Applications, 2013; 3: 820-827.

[3] Manjaree S, Agarwal V and Nakra B C. Kinematic Analysis Using Neuro-Fuzzy Intelligent Technique for Robotic Manipulator. International Journal of Engineering Research and Technology, 2013; 6: 557-562.

[4] Al-Faiz Z M and Salesh S M. Inverese Kinematic Analysis for Manipulator Robot with Wrist Offest Based on the Closed Form Algorithm. International Journal of Robotics and Automation, 2011; 2.

[5] Eliot E, Deepak B B V L, Parhi D R and Srinivas J. Design & Kinematic Analysis of an Articulated Robotic Manipulator.

[6] Chang Y, Ma S, Wang H and Tan D. A Kinematic Modelling Method for a wheeled mobile robot. International Conference on Mechatronics and Automation, 2009.

[7] Manjunath T C. Kinematic Modelling of Maneuvering of A 5-Axes Articulated Robot Arm. International Journal of Mechanical, Aerospace, Industrial and Mechatronics Engineering .2007; 1: 4.

[8] Zarkandi S and Esmaili M R. Direct Position Kinematics of a Three Revolute Prismatic-Spherical Parallel Manipulator. International Journal of Research and Reviews in Applied Sciences,2011; 7: 1.

[9] He B, Han L, Wang Y, Huang S and Liu L. Kinematic analysis and numerical simulation of a manipulator based on virtual prototype. Int J Adv Manuf Technol, 2014:7:943-963.

[10] Kalyoncu M .Mathematical modelling and dynamic Response of a Multi Straight-line path tracing flexible robot manipulator with rotating-prismatic joint. Applied Mathematical Modelling, 2008; 32: 1087-1098.

[11] Hussien M T, Al-Robaiy M J and Al-Shjary M A. Mathematical Modelling of flexible Robotic Arm using Finite Element Method.

[12] Tokhi M O and Mohamed Z. Finite element approach to dynamic modelling of a flexible robot manipulator: performance evaluation and computational requirements. Communications in Numerical Methods in Engineering, 1999; 15: 669-678.

[13] Ahmad M A, Zawawi M A and Mohamed Z. Effect of Beam's Length on the Dynamic Modelling of Flexible Manipulator System. 11th International Conference on Computer Modelling and Simulation , IEEE , 2009: 356-361.

[14] Loudini M, Boukhetala D, Tadjine M and Boumehdi M. A. Application of Timoshenko Beam Theory For Deriving Motion Equations of a Lightweight Elastic Link Robot Manipulator. International Journal of Automation, Robotics and Automomous System 2006; 05(2): 11-18.

[15] KhalilIbrahim, Aly A A and Ismail A A. Mode shape analysis of a flexible robot arm. International Journal of Control, Automation and Systems, 2013; 1: 2.

[16] Korayam M H, Shafei A M and Dehkordi S F. Dynamic effect of beam's length and beam's theory on the flexible manipulator system. International Research Journal of Applied and Basic Sciences, 2012; 3: 1527-1534.

[17] Oguamanam B, Bošnjak S and Zrnić N. On the dynamic modelling of flexible manipulators. FME Transactions, 2006; 34: 231-237.
[18] Wang P K C and Wei J. Vibration in a moving flexible robot arm. Journal of sound and vibration, 1987; 1: 149-160.
[19] Zohoor H and Kakavand F. Timoshenko versus Euler-Bernoulli beam theories for high speed two-link manipulator. Scientia Iranica B, 2013; 1: 172-178.
[20] Gripp J A B, Santos F L M, Bernardos C R and Goes L C S. Modelling and identification of a two link flexible manipulator. ABCM Symposium Series in Mechatronics, 2012; 5: 1092-1101.
[21] Chen W. Dynamic modelling of multi-link flexible robotic manipulators. Computers and Structures, 2001; 79: 183-195.
[22] Theodore R J and Ghosal A. Comparison of the assumed mode and finite element models for flexible multi- link manipulators. The International Journal of Robotics Research, 1995; 2: 91-111.
[23] Shanker M C and Ghosal A. Nonlinear modelling of flexible manipulators using non-dimensional vairables.
[24] Pratap D and Reddy Y V M. Kineto-Elasto dynamic analysis of robot manipulator puma-560. Journal of Mechanical and Civil Engineering, 2013; 8: 33-40.
[25] Torby J B and Kimura I. Dynamic modelling of a flexible manipulator with prismatic links. Journal of Dynamic Systems, Measurement, and Control, 1999; 121: 691-696.
[26] Al-bedoor B O and Khulief Y A. Finite element dynamic modelling of a translating and rotating flexible link. Computer Methods in Applied Mechanics and Engineering, 1996; 131: 173-189.
[27] Tokhi M O, Azad A K M, Poerwanto H, Kourtis S and Baxter M J. A Simulink Environment for Simulation and Control of Flexible Manipulator Systems. International Conference on Control, 1996; 427: 2-5.
[28] Yih E Y S. Vibration suppression of a flexible manipulator using adaptive input shaping
[29] Akyuz I H, Bingul Z and Kizir S. Cascade fuzzy logic control of a single-link flexible-joint manipulator. Turk J Elec Eng & Comp Sci, 2012; 31: 713-726.
[30] Mohamed Z and Tokhi M. O. Command shaping techniques for vibration control of a flexible robot manipulator. Mechatronics, 2004; 14: 69-90.
[31] Sa'id W K, Kazem B I and Manaty A M. Hybrid Controller for a single flexible link manipulator. Journal of Engineering, 2012; 12: 1242-1254.
[32] Shaheed M H, Tokhi M O, Chipperfeild A J and Azad A K M. Modelling and open-loop control of a single link flexible manipulator with genetic algorthims. Journal of Low Frequency Noise, Vibration and Active Control, 2001; 20: 39-55.
[33] Subudhi B and Morris A S Dynamic modelling, simulation and control of a manipulator with flexible links and joints. Robotics and Autonomous Systems, 2002; 41: 257-270
[34] Zebin T and Alam M S. Modelling and Control of a Two Link Flexible Manipulator using Fuzzy Logic and Genetic Optimization Techiniques. Journel of Computers, 2012; 7 : 578-585.
[35] Bottega V, Pergher R, Molter A and Fonseca J O. Optimization of piezoelectric actuator for manipulator with non-prismatic links, International Conference on Engineering Optimization, 2008.
[36] Rigatos G G. A Robust nonlinear control approach for flexible-link robots using kalman filtering. Cybernetics and Physics, 2012; 1: 134-143.

[37] Shan J, Liu T H and Sun D. Modified input shaping for a rotating single-link flexible manipulator, Journal of Sound and Vibration, 2005; 285: 187-207.
[38] Tang Y G, Sun F C, Sun Z Q and Hu T H. Tip Position Control of a Flexible-Link Manipulator with Neural Networks. International Journal of Control, Automation, and Systems, 2006; 4: 308-317.
[39] Kuo C F J and Lin S C. An entire strategy for precise system tracking control of a revolving thin flexural link, Part I: Finite Element Modelling and Direct Tuning Controller Design. Mathematical and Computer Modelling, 1999; 29: 99-113.
[40] Kazi S and Mansour T M. Fuzzy Logic Modified Proportional-Integral-Derivative (MPID) Control for Flexible Manipulator. International Journal of Circuits, Systems and Signal Processing, 2013; 7: 285-293.
[41] Wang Z, Zeng H, Ho D W C and Unbehauen H. Multi objective Control of a Four-Link Flexible Manipulator: A Robust H Approach. IEEE Transactions on Control Systems Technology, 2002; 10: 866-875.
[42] Chang M Y, Chen J K and Chang Y C. A simple spinning laminated composite shaft model. Int. Journal of Solids and Structures, 2006; 41(3-4): 637-662.
[43] Roy T and Chakraborty D. Delamination in Hybrid FRP Laminates under Low Velocity Impact. Journal of Reinforced Plastics and Composites, 2006; 25(18): 1939-1956.